Aus dem
Walther-Straub-Institut
für Pharmakologie und Toxikologie
der Ludwig-Maximilians-Universität München

Vorstand: Prof. Dr. med. Thomas Gudermann

Transient Receptor Potential A1 Channels and Their Role in the Cytotoxicity of Sulfur Mustard

Kumulative Dissertation
zum Erwerb des Doktorgrades der Naturwissenschaft
der Medizinischen Fakultät
der Ludwig-Maximilians-Universität zu München

vorgelegt von
Bernhard Stenger

aus
Homburg

2017

Mit Genehmigung der Medizinischen Fakultät
der Universität München

Betreuer:	Privatdozent Dr. med. Dr. rer. nat. Harald Mückter
Zweitgutachter:	Professor Dr. Gerhard Scherer
Dekan:	Professor Dr. med. dent. Reinhard Hickel

Tag der mündlichen Prüfung: 11.07.2018

Contents

Eidesstattliche Versicherung

Ich erkläre hiermit an Eides statt, dass ich die vorliegende Dissertation mit dem Thema „Transient Receptor Potential A1 Channels and Their Role in the Molecular Toxicology of Sulfur Mustard“ selbständig verfasst, mich außer der angegebenen keiner weiteren Hilfsmittel bedient und alle Erkenntnisse, die aus dem Schrifttum ganz oder annähernd übernommen sind, als solche kenntlich gemacht und nach ihrer Herkunft unter Bezeichnung der Fundstelle einzeln nachgewiesen habe.

Ich erkläre des Weiteren, dass die hier vorgelegte Dissertation nicht in gleicher oder in ähnlicher Form bei einer anderen Stelle zur Erlangung eines akademischen Grades eingereicht wurde.

München, den 21.11.2017

_____
(Bernhard Stenger)

Abstract

The chemical warfare agent sulfur mustard (SM), which is also known as *'mustard gas'*, exhibits a malodorant mustard- or garlic-like odor. Recognition of odors is part of the physiological chemosensation, a process that describes the transduction of chemical signals into biological perception. This process has been shown to rely on Transient Receptor Potential cation-channels (TRP-channels). Especially TRPA1 channels have been found to respond to a plethora of reactive noxious compounds, including pungent substances like allyl-isothiocyanate or mustard oil. Additionally, pain and itch, two clinical symptoms in SM poisoning, are connected to TRPA1 activation. However, whether SM targets TRPA1-channels has not been investigated so far and is the main subject of the presented thesis.
After establishment of a HEK cell line overexpressing functional human TRPA1 channels, intracellular Ca^{2+} ($[Ca^{2+}]_i$) was measured as indicator of TRPA1 activation. However, SM interfered with conventional AM-esters (Fura-2). Thus, apoaequorine was used to investigate changes in $[Ca^{2+}]_i$. Subsequently, we were able to prove activation of TRPA1 by SM in a dose-dependent manner. Remarkably, SM cytotoxicity was found enhanced in cells overexpressing TRPA1, and use of specific TRPA1 blockers counteracted this effect.
The second part of the presented thesis focuses on the activation mechanism of TRPA1 channels by alkylating compounds. Release of reactive oxygen species (ROS) has been demonstrated to be a key event in SM cytotoxicity. As TRPA1 can be activated by ROS, we investigated the impact of well-established ROS scavengers (*N*-Acetyl-L-cysteine (NAC) and glutathione (GSH)) in regard to SM-induced TRPA1 activation. NAC prevented Ca^{2+} influx after SM-application whereas GSH did not. A direct scavenging of SM by NAC could be ruled out by LC-ESI MS/MS analysis. This suggests that NAC interacts with TRPA1 moieties not accessible to GSH, thereby modulating channel function.

Our results demonstrated that TRPA1 channels are activated by alkylating compounds. However, the cellular effects remain unclear and should be addressed in future studies. Activation of MAP kinases, which has also been described after SM exposure, is also a downstream target of TRPA1 activation and represents a promising field of research. Moreover, the exact mechanism of SM-induced TRPA1 activation remains unresolved so far. TRPA1 mutants, lacking possible alkylation sites, are to be established to identify the relevant residues in TRPA1 channels.
The role of TRPA1 in SM pathophysiology has to be further elucidated. After SM exposure, patients frequently report tautness in combination with severe itch, inflammation and wound healing disorders, which can be connected to TRPA1-dependent signaling pathways. Thus, TRPA1-blockers may be of benefit to relief some of the above-mentioned symptoms.

Kurzfassung

Der chemische Kampfstoff Schwefel-Lost (S-Lost) weist einen stechenden, senf- oder knoblauchartigen Geruch auf, was zum Synonym „Senfgas“ führte. Das Wahrnehmen von Gerüchen ist Teil der physiologischen Chemosensorik - ein Prozess, der die Transduktion von chemischen Signalen in eine biologische Antwort beschreibt. *Transient Receptor Potential* (TRP) Kanäle wurden hier als wichtige Akteure identifiziert. Insbesondere konnten TRPA1 Kanäle als entscheidend bei der Detektion von hochreaktiven und giftigen Substanzen, einschließlich Reizstoffen wie z. B. Allylisothiozyanat oder Senföl, nachgewiesen werden. Weiterhin wird TRPA1 eine wichtige Rolle bei Schmerz und Juckreiz – beides Symptome, die auch nach einer S-Lost Exposition auftreten – zugeschrieben. Ob auch alkylierende Substanzen TRPA1 Kanäle aktivieren können, wurde bisher nicht untersucht und ist Gegenstand der vorgestellten Dissertation.
Nach der Etablierung einer hTRPA1-überexprimierenden HEK Zelllinie wurde die Kanalaktivierung durch Messung der intrazellulären Ca^{2+} Konzentration bestimmt. Eine Interaktion zwischen S-Lost und den für Ca^{2+} Messungen gebräuchlichen Fura-2 Farbstoff wurde nachgewiesen. Für die weiteren Versuche wurde daher eine Apoaequorin-Methode genutzt. Mit dieser gelang der Nachweis einer TRPA1-Aktivierung durch S-Lost. Zusätzlich zeigten sich diese Zellen signifikant empfindlicher gegenüber S-Lost. TRPA1-Blocker konnten die Zytotoxizität deutlich abmildern. Im zweiten Teil der Dissertation wurde der Mechanismus einer S-Lost-induzierten TRPA1-Aktivierung genauer untersucht. Die Freisetzung reaktiver Sauerstoffspezies (ROS) ist essentieller Bestandteil der Zytotoxizität von S-Lost. ROS können TRPA1 Kanäle aktivieren, weshalb der Einfluss zweier etablierter ROS-scavenger (*N*-Acetyl-l-cysteine (NAC) und Glutathion (GSH) auf die S-Lost-induzierte TRPA1-Aktivierung untersucht wurde. NAC konnte den Ca^{2+}-Einstrom wirkungsvoll verhindern, während GSH keinen Effekt zeigte. Eine Bildung von Addukten zwischen S-Lost und NAC oder GSH konnte mittels LC-ESI MS/MS ausgeschlossen werden. Dementsprechend wurde eine Interaktion zwischen NAC und extrazellulären TRPA1-Anteilen postuliert, die eine Modulation der Kanalfunktion zur Folge hat.

Unsere Ergebnisse belegen, dass alkylierende Substanzen TRPA1-Kanäle aktivieren können. Jedoch sind die zellulären Konsequenzen noch unklar. Die Aktivierung von MAP-Kinasen, die auch nach S-Lost Exposition beschrieben wurde, kann Folge einer TRPA1-Aktivierung sein. Weitere Untersuchungen sind hier notwendig. Der TRPA1-Aktivierungsmechanismus durch S-Lost ist nicht vollständig verstanden. Dieser könnte durch TRPA1-Mutanten, bei denen mögliche Bindestellen fehlen, weiter aufgeklärt werden. Nach einer S-Lost Exposition klagen Patienten über Spannungsgefühl der Haut, starken Juckreiz, Entzündung und Wundheilungsstörungen. Für diese Symptome wird ein Zusammenhang zu TRPA1-gesteuerten Signalkaskaden diskutiert. Der Einsatz von TRPA1-Blockern könnte daher eine therapeutische Option nach S-Lost Exposition darstellen.

List of Figures

List of Publications

Original Research Articles Presented in This Thesis

Bernhard Stenger, Franziska Zehfuß, Harald Mückter, Annette Schmidt, Frank Balszuweit, Eva Schäfer, Thomas Büch, Thomas Gudermann, Horst Thiermann, Dirk Steinritz (2015). Activation of the chemosensing transient receptor potential channel A1 (TRPA1) by alkylating agents. *Archives of Toxicology*, 89, 1631-1643.

Bernhard Stenger, and Tanja Popp, Harald John, Markus Siegert, Amelie Tsoutsoulopoulos, Annette Schmidt, Harald Mückter, Thomas Gudermann, Horst Thiermann, Dirk Steinritz (2016). N-acetyl-L-cysteine inhibits sulfur mustard-induced and TRPA1-dependent calcium-influx *Archives of Toxicology*, 91, 2179-2189.

Original Research Articles

Marina Schäfer, Franziska Koppe, **Bernhard Stenger**, Christoph Brochhausen, Annette Schmidt, Dirk Steinritz, Horst Thiermann, Charles James Kirkpatrick, Christine Pohl (2013). Influence of organophosphate poisoning on human dendritic cells. *Chemical-biological interactions*, 206, 472-478

Dirk Steinritz, Niklas Möhle, Christine Pohl, Mirko Papritz, **Bernhard Stenger**, Annette Schmidt, Charles James Kirkpatrick, Horst Thiermann, Richard Vogel, Sebastian Hoffmann, Michaela Aufderheide (2013). Use of the Cultex® Radial Flow System as an in vitro exposure method to assess acute pulmonary toxicity of fine dusts and nanoparticles with special focus on the intra- and inter-laboratory reproducibility. *Chemical-biological interactions*, 206, 479-490

Dirk Steinritz, Franziska Zehfuß, **Bernhard Stenger**, Annette Schmidt, Tanja Popp, Kai Kehe, Harald Mückter, Horst Thiermann, Thomas Gudermann (2017). Zinc chloride-induced TRPA1 activation does not contribute to toxicity in vitro. *Toxicology Letters*, epub ahead of print

Proceedings & Poster Presentations

Marina Schäfer, Christine Pohl, **Bernhard Stenger**, Dirk Steinritz, Charles James Kirkpatrick (2013). Influence of organophosphates on a bronchial triple culture. *Naunyn-Schmiedeberg's Archives of Pharmacology* 386, S70 (2013).

Dirk Steinritz, **Bernhard Stenger**, Franziska Zehfuß, Harald Mückter, Annette Schmidt, Frank Balszuweit, Thomas Richard Heinrich Büch, Andreas Breit, Horst Thiermann, Thomas Gudermann (2015). Alkylating agent (Sulfur Mustard) induced calcium influx is TRPA1 dependent. *Naunyn-Schmiedeberg's Archives of Pharmacology* 388, S8-S9 (2015).

Bernhard Stenger, Andreas Breit, Tanja Popp, Horst Thiermann, Thomas Gudermann, Dirk Steinritz (2016). Alkylating agents activate MAPK signaling through TRPA1. *82nd Annual Congress of the German Society of Experimental and Clinical Pharmacology and Toxicology (DGPT)*, Berlin, 2016.

Bernhard Stenger, Dirk Steinritz, Amelie Tsoutsoulopoulos, Andreas Breit, Horst Thiermann, Annette Schmidt, Harald John, Tanja Popp, Thomas Gudermann (2016). Alkylating agents activate chemosensing Transient Receptor Potential A1 cation channels. *52nd European Congress of the European Societies of Toxicology*, Seville, 2016.

Thomas Guderman, **Bernhard Stenger**, Franziska Zehfuß, Alexander Dietrich, Andreas Breit, Harald Mückter, Harald John, Annette Schmidt, Tanja Popp, Horst Thiermann, Dirk Steinritz (2016). Activation of TRPA1 channels by alkylating agents and zinc chloride. *Wehrmedizinische Monatsschrift 60*, S3-S4 (2016).

Bernhard Stenger, Dirk Steinritz, Amelie Tsoutsoulopoulos, Andreas Breit, Horst Thiermann, Annette Schmidt, Harald John, Tanja Popp, Thomas Gudermann (2016). Alkylating agents activate chemosensing TRPA1 cation channels. *Toxicology Letters 258S*, S245 (2016).

Dirk Steinritz, **Bernhard Stenger**, Tanja Popp, Andreas Breit, Horst Thiermann, Thomas Gudermann (2016). Activation of TRPA1 channels by alkylating agents. *Advances & Breakthroughs in Calcium Signaling*, Honolulu, 2016.

Amelie Tsoutsoulopoulos, **Bernhard Stenger**, Thomas Gudermann, Andreas Breit, Horst Thiermann, Annette Schmidt, Harald John, Tanja Popp, Dirk Steinritz (2016). TRPA1-Aktivierung durch alkylierende Verbindungen. *Deutsche Gesellschaft für Wehrmedizin und Wehrpharmazie*, Neu-Ulm, 2016.

Bernhard Stenger, Tanja Popp, Harald John, Markus Siegert, Amelie Tsoutsoulopoulos, Annette Schmidt, Harald Mückter, Horst Thiermann, Thomas Gudermann, Dirk Steinritz (2017). Effect of N-Acetyl-L-Cysteine and Glutathion on Alkylating Agents-induced TRPA1-Channel Activation. *16th Medical Chemical Defense Conference*, München, 2017.

Alexander Dietrich, Martina Kannler, Susanne Fiedler, Jonas Weber, Tanja Popp, **Bernhard Stenger**, Harald Mückter, Dirk Steinritz, Horst Thiermann, Thomas Gudermann. Molecular findings in toxic lung injury. *16th Medical Chemical Defense Conference*, München, 2017.

Bernhard Stenger, Tanja Popp, Annette Schmidt, Thomas Gudermann, Horst Thiermann, Dirk Steinritz. Gibt es einen Schwefel-Lost-Chemosensor? *Wehrmedizinische Monatsschrifft*, Sonderdruck "Heinz-Gerngroß-Förderpreis 2017", 2017.
Awarded with the "Heinz-Gerngroß-Förderpreis 2017".

1 Introduction

1.1 Sulfur Mustard - Historical Background

The exact date of the initial sulfur mustard (SM, bis(2-chlorethyl)sulfide, CAS-Nr. 505-60-2) synthesis is unknown. A number of reports mention the preparation of an oily liquid, which should later be named SM, by the Belgian-French scientist César-Mansuète Despretz in 1822 [1]. Some 100 years after this event, Fritz Haber suggested the use of chemicals – initially chlorine and phosgene – as warfare agents in World War I (WWI). Willhelm Lommel, employee of the *Bayer Chemical Works* in Leverkusen, and Wilhelm Steinkopf, head of the *Chemical Weapons Research Unit* at the Kaiser Wilhelm Institute of Physical Chemistry and Electrochemistry in Berlin, were both co-workers of Fritz Haber. They developed a large-scale SM production process that allowed synthesis of the agent. This circumstance accomodated for the acronym *'S-Lost'* that resembles the initials of both chemists [1]. Whereas the use of chemical weapons, e.g. in the Middle East, is presently regarded with abhorrence, chemical warfare had many supporters during WWI [2]. Convential warfare, killing thousands of soldiers by artillery or hand-to-hand combat, for example during the battle of Verdun in which more than 700.000 soldiers were either wounded or killed, was regarded as inhumane [3]. Moreover, supply with conventional ammunition ran short. All these were reasons for the initiation of chemical warfare. Chlorine gas was the first chemical that was deployed during the 2nd battle of Ypres on April 22nd 1915 and, thereby, historically marked the beginning chemical warfare. Two years later, almost at the end of WWI, SM was the last chemical agent to be introduced into war, again in Ypres [4]. Over a 10 day period about one million shells containing more than 2,000 tons of SM were delivered by the Germans [2]. In total, some 9 million SM-containing artillery shells were fired by all warring parties during WWI resulting in a total of around 400,000 casualties [2, 5]. Not being lethal in first line, SM led to injuries of multiple organs including the respiratory tract. It was considered as potent warfare agent and, thus, became known as the *'king of battle gases'* [2, 6].
In the wake of WWI chemical warfare agents, including SM, were forbidden by the Geneva Protocol [7]. However, violations of that agreement were reported, and SM was used in several conflicts including the Rif War in Morocco in the early 1920s, during the Soviet invasion of Xinjiang in 1934, or by Italian soldiers in Lybia in the aftermath of the Italo-Turkish war in 1930 [8, 9, 10]. Fortunately, SM was not – or only in some very rare events – used in World War II (WWII). However, there is some evidence underlining the awareness of its occasional use: during the Bari incident on December 2nd 1943, the US Navy ship SS John Harvey, carrying some hundred tons of SM, was sunk by the German Air Force. During this incident the toxic substance was released and about 650 people were exposed [5].
More recently, severe deployment of SM took place in the Kurdish city Halabdscha in Iraq in 1988 when Ali Hasan al-Madschid al-Tikriti, cousin of the former Iraqi dictator Sadam Hussein, issued the order to deploy nerve agents, cyanids and SM on Kurdish civilians. In 2010, so-called *'Chemical-Ali'* was sentenced to four times death for that crime [11, 12]. The latest use of SM, most probably by ISIS or other terroristic groups, was reported in connection with the ongoing Syria conflict. Photographs of grenades revealing leakage of a black liquid and casualties that were close to the spot

at Cobane exhibiting typical clinical symptoms of SM poisoning can be found on the internet (Figure 1.1). Meanwhile the Organisation for the Prohibition of Chemical Weapons (OPCW) confirmed the use of SM in Syria from 2013 until present [13].

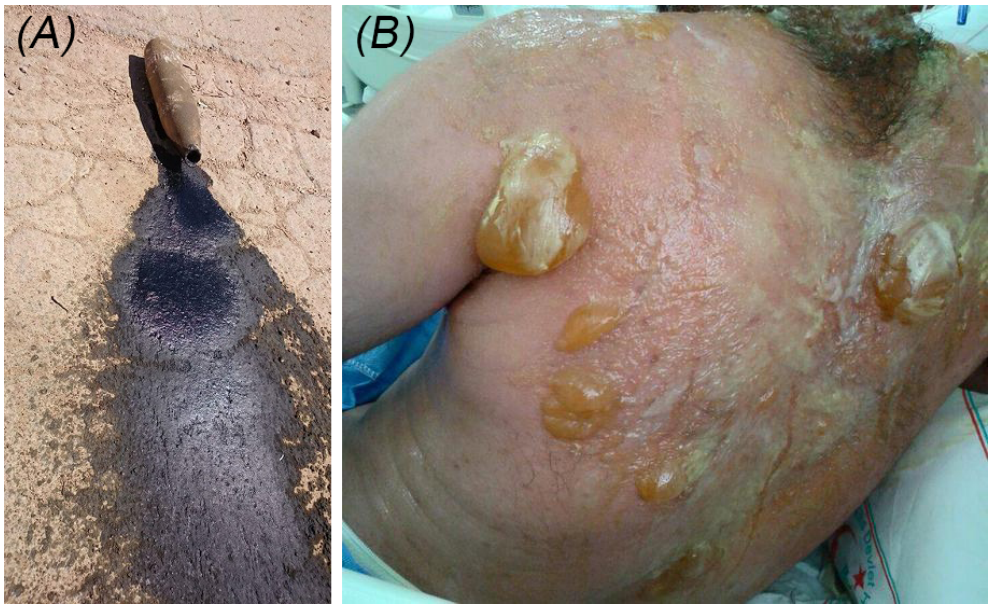

Figure 1.1: SM-containung artillery shell and SM-exposed patient. (A) Photograph showing an artillery shell with leakage of an oily liquid, most likely SM, taken on September 1st 2015 near Cobane (Syria) [14]. (B) Photograph of an in-patient, exhibiting typical clinical symptoms of SM poisoning, recorded on September 3rd 2015 near Aleppo [14].

1.2 Clinical Picture of Sulfur Mustard Poisoning

SM causes severe damage to every exposed organ and tissue. Most common are acute adverse health effects of the dermal, respiratory and ocular systems [5, 15, 16, 17]. Systemic symptoms may also develop. The perfidious characteristics of SM had already been recognized by Albert Niemann in 1860: 'They are represented by the fact that even traces when brought into contact with the skin, while painless at first, result in a reddening of the skin after several hours, and in subsequent days form blisters which fester and heal slowly and with great difficulty, leaving behind significant scarring' [18]. Unnoticed at first, skin irritations including tautness, itch, erythema will develop usually within 2 - 3 hours after contact with the agent, but may also take up to 24 h [5, 16, 17]. On affected skin areas blisters develop leading to extensive ulceration. These SM-induced skin wounds are characterized by wound healing disorders, which frequently necessitate skin transplantation.

Unprotected eyes are the most sensitive organ with regard to airborne SM exposures. Symptoms will develop within 1 - 2 h, depending on the SM exposure dose. Pain,

photophobia and blepharospasms are common [15, 17]. Corneal damage, which may even occur decades after a single exposure event, is feared [19].
Pulmonary exposure with SM-aerosols may be life-threatening. SM is able to reach lower lung compartments, i.e. the alveolar region, due to its poor water solubility [20]. In principle, a toxic reaction comparable to the skin lesions can be observed: lung epithelial cells detach, mix with mucus and exsudate therby forming diphtheria-like pseudomembranes that clot and obstruct the airways [17, 21]. This, unless immediately treated by broncho-alveolar lavage and intensive care measures, results in asphyxia in most cases.

Unfortunately, neither a specific antidote nor specific therapeutic measures are available. One reason is the largely unkown cytotoxicity of SM. Early decontamination, at least of affected areas, is of utmost importance to prevent further uptake of the agent. Sodium or calcium hypochlorite solutions or powders may be used to accelerate SM hydrolysis or oxidation to harmless products. [5]. More recently, RSDL (reactive skin decontamination solution) was introduced for decontamination purposes [22].
Malignancies of the lung, skin and blood marrow are examples of long-term health effects after SM exposures and have been frequently reported [16, 23, 24]. Despite all the adverse effects that SM has caused while being abused as CWA, physicians have also recognized its toxic potential to fight malignant cells and tissue. During WWI scientists realized that SM has antiproliferative effects [25]. After WWII, Nitrogen Mustards were developed. These were less toxic but had similar effects regarding the inhibition of proliferation, leading to the first cytostatic agents and the start of the era of alkylation chemotherapy. A plethora of alkylating compounds were synthesized including chlorambucil, melphalan, or bendamustine [26]. Some of these early cytostatic agents are still in use in current cancer therapy.

1.3 Molecular Toxicology

The highly reactive SM is able to alkylate a plethora of biomacromolecules including DNA. SM-DNA-adducts, especially interstrand crosslinks, have long been regarded as the main reason for toxicity. However, these damages can be repaired by nucleotide excision repair (NER) or base excision repair (BER) processes [27, 28]. Thus, other mechanisms are most likely to be involved in the molecular toxicology. The chemical reaction mechanism has been precisely explored: intramolecular nucleophilic substitution leads to the elimination of a chloride ion resulting in the formation of a cyclic sulfonium ion. This highly reactive intermediate cause covalent modifications of different biomolecules including DNA (Figure 1.2, p. 4).

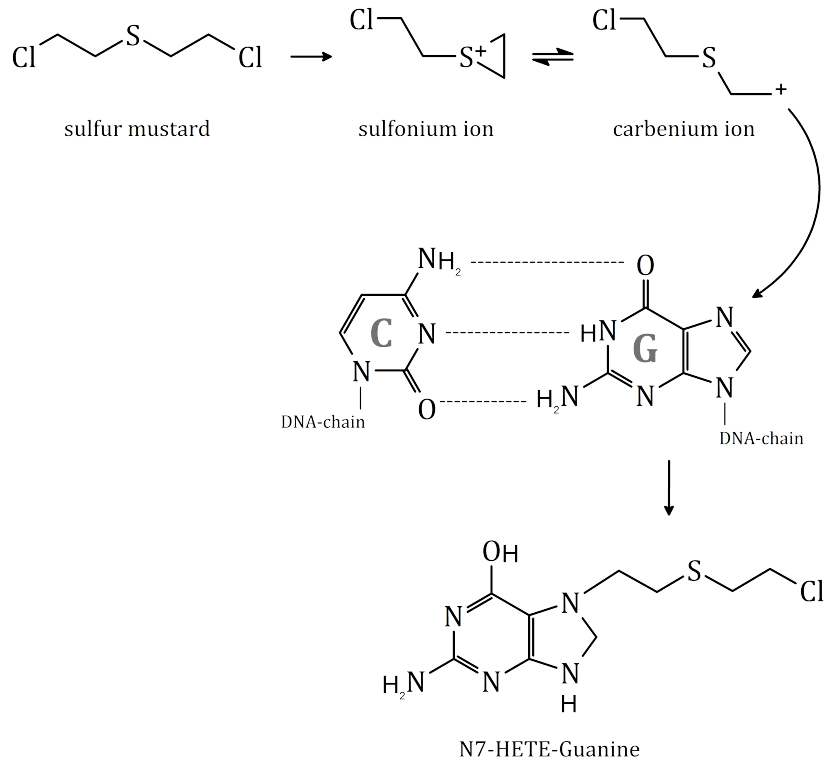

Figure 1.2: SM induced DNA alkylation at guanine residues. First, in aqueous environments SM forms a sulfonium ion which is then transformed into a carbenium ion. This highly reactive intermediate binds to N7 residues of guanine bases resulting in N7-HETE-G. 'C' represents cytosine, and 'G' respresents guanine residues.

Different mono- and bi-functional DNA-adducts at guanine and adenine residues have been described [29, 30]. Some of these adducts can be excised by different DNA repair mechanisms, like BER or NER, whereas O6-[2-[(2-hydroxyethyl)thio]ethyl]-guanine cannot be repaired and, therefore promotes mutagenesis. Altough the alkylation of DNA is the most common lesion, the carbenium ion can also react with many nucleophils such as O, S, or N, which are part of amino acids, enzymes, co-enzymes, structural proteins, or earlier mentioned nucleic acids. During both hydrolysis and alkylation reactions of SM, different chemical byproducts, such as e.g. H^+, emerge. These may also contribute to toxicity. SM is well known to cause oxidative (ROS) and nitrosative (RNS) stress. ROS play a crucial role in cell signaling and homeostasis, although increasing amounts can override cellular defense systems and thus cause pathological states [31, 32]. The formation of ROS, especially superoxide and hydroxyl radicals, can be counteracted by antioxidative compounds like GSH [33]. GSH has been shown to act as SM scavenger *in vitro*, however, by depleting antioxidants [34]. Furthermore, it has been reported that antioxidative enzymes are inhibited by SM, thereby elevating ROS and aggravating cell damage [35]. Both, excessive DNA alkylation in combination with increased alkylation and loss of essential cellular cofactors (i.e. NAD^+, ATP) may trigger cell death. Various modes of cell death have been described: uncontrolled necrosis, a more or less

uncontrolled disintegration of cells, and programmed cell death, called apoptosis. Additionally variations of programmed cell death are necroptosis and authopagy. In case of necroptosis, different death receptors are activated and thereby promote cell death. Although being triggered by the cell itself, proteins are not cleaved in a controlled manner, instead necrotic disintegration is the case [36]. Autophagy describes a controlled degradation of malfunctioning proteins and cellular parts. The resulting morphology can be differentiated from apoptosis [37]. Apoptosis is executed by the sequential activation of different caspases. Activated effector caspases, e.g. caspase-3, will finally cleave different substantial proteins. Degradation products become embedded in apoptotic bodies which are cleared by efferocytosis, thereby preventing any release of cytoplasmic matter into the extracellular environment [38, 39]. In contrast to apoptosis, necrosis results in inflammation because of uncontrolled release of cytoplasmic contents from disrupted cells [40, 41]. For SM both necrosis and apoptosis have been described [42, 43, 44, 45]. Necrosis is observed after high doses of SM, whereas apoptosis takes place at lower doses of SM. Erythema and inflammation, most probably due to necrosis but also linked to the release of pro-inflammatory cytokines, have been frequently observed after SM exposures. Along with the release of pro-inflammatory IL6, IL8, or TNFα, leukocytes increase in number [44, 46]. Furthermore, an upregulation of pro-inflammatory proteins, like cyclooxygenase, inducible nitric oxide synthase, or myeloperoxidase was found after SM exposure [47]. Based on decades of research, it has to be assumed that the toxicity of SM is not attributed to a single but rather to a plethora of different toxicological mechanisms. Obviously, SM can be sensed. A malodorant, pungent, mustard- or garlic-like odor was already noticed by Despretz. This typical smell was eponymous for the term ‘mustard gas’, although misleading as SM is not gaseous at room temperature. Whether pure SM, its hydrolysis products or impurities during the synthesis process all exhibit this characteristic is a matter of controversial debate. However, the specific odor was used as an indicator of SM deployment as illustrated on many warning and information notices (Figure 1.3).

Figure 1.3: SM warning and information notices from World War II. Posters served to warn soldiers and civilians about the feared use of chemical warfare agents. Here, the characteristic odor of SM is addressed [48, 49].

1.4 Chemosensation

Chemosensation, also known as chemoreception, is the ability to perceive chemicals. Beside, some authors also include the perception of (noxious) cold or heat in the definition of chemoreception. Chemoreceptors were initially discovered in the nasal mucosa and in the oral taste bulbs. They were found to be essential for distinguishing different flavors. The receptor for bitter-tasting 'chemicals' is the G protein-coupled receptor TAS2Rn [50]. Interestingly, these receptors are also expressed in the motile cilia of the airway epithelium [50]. Another example of peripheral chemoreceptors are carotid bodies that sense e.g. oxygen levels in the blood and translate the information to a neuronal output with subsequent adaptation of respiration [51]. More recently, nasal trigeminal nerve endings were described to be also particularly sensitive to highly toxic chemicals, i.e. chlorine [52]. A plethora of proteins were identified being involved in the physiological process of chemosensation. However, immediate changes of intracellular ion levels, i.e. increase of intracellular calcium levels ($[Ca^{2+}]_i$), seem to be key events. Likely candidates involved in this Ca^{2+} influx phenomenon are members of the transient receptor potential channel (TRP channels) family.

1.4.1 Transient Receptor Potential Ion Channels

TRP channels are a heterogenous group of ion channels. Depending on the species, up to about 30 TRP channels have been described which share several structural similarities. The superfamily of TRP-channels consists of seven subfamilies: canonical TRP channels (TRPC), vanilloid TRP channels (TRPV), melastatin TRP channels (TRPM), mucolipin TRP channels (TRPML), polycystin TRP channels (TRPP),

no-mechanoreceptor potential channels (NOMPC = TRPN), and TRPA channels with the sole member ANKTM1 (Figure 1.4).

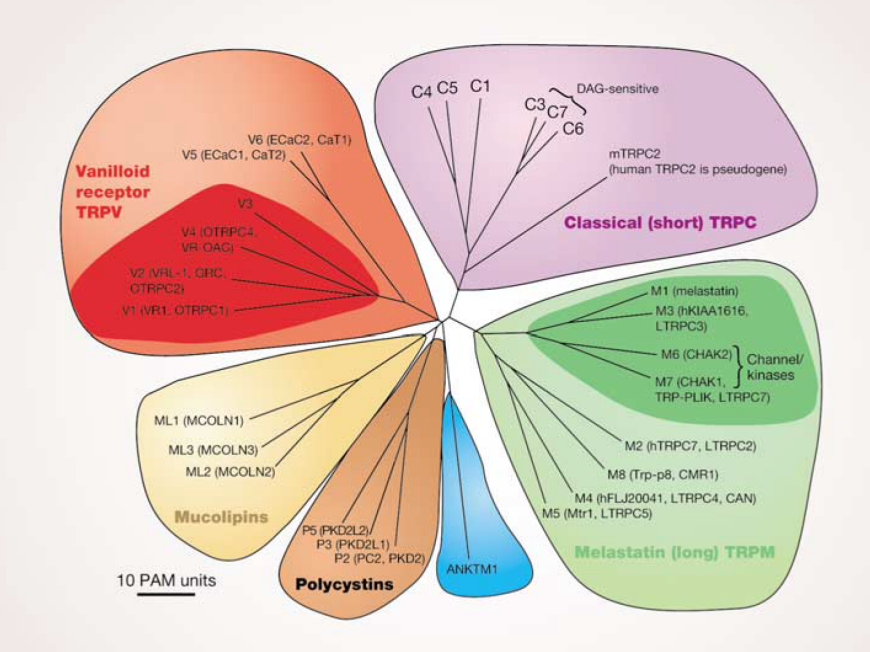

Figure 1.4: Phylogenetic tree of the TRP-channel superfamily [53].

In general, all TRP channels are composed of 6 transmembrane domains [54]. Both N- and C-termini are located inside the cytosol. Numerous protein modifications including phosphorylation, ubiquitination or protein-protein interaction, e.g. G protein receptor coupling or ligand gating, have been described. A cation-permeable pore region is located between the transmembrane domains 5 and 6 (Figure 1.5) [54]. It is suggested that a functional unit is formed by 4 TRP channels. Heteromeric, as well as homomeric tetramers have been described, depending on the type of the TRP channel.

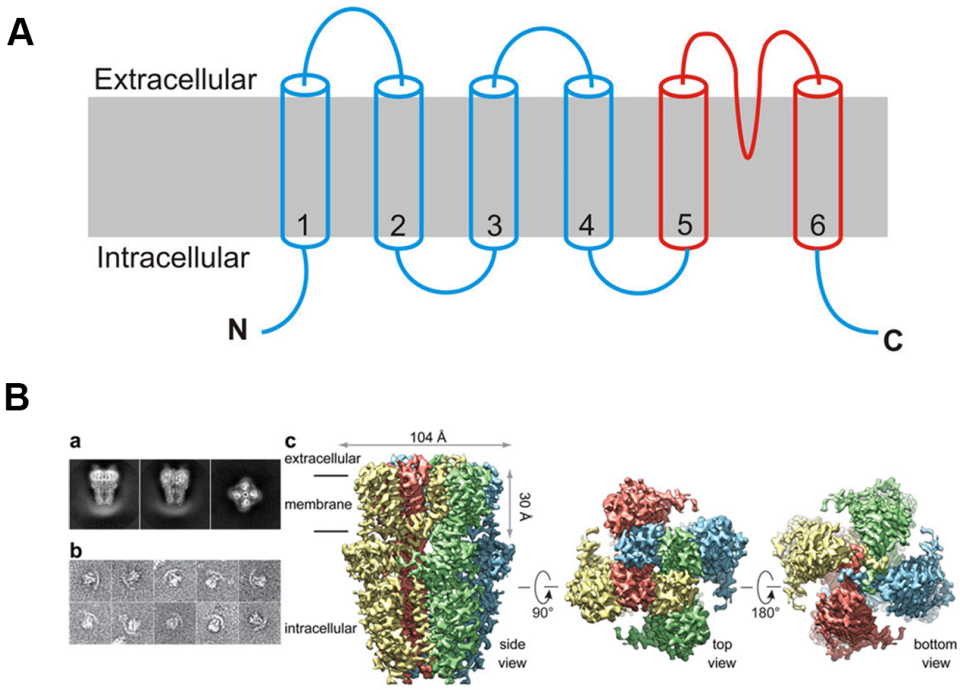

Figure 1.5: Structure and constitution of TRP channels. (A) Transmembrane topology of the ion channel subunits. TRP channels consist of six transmembrane domains. A pore region is formed between S5 and S6 [55]. (B) Crystal structure of the human TRPA1 tetramer [56].

Many of these channels mediate a variety of sensations like the sensations of pain and hotness, sensitivity to warmth or cold, different kinds of tastes, pressure, and vision [52, 54, 57, 58, 59, 60, 61]. Specific activators of certain TRP channels were identified: some channels are activated by the garlic ingredient allicin (TRPA1 & TRPV1), capsaicin (TRPV1), or the wasabi ingredient allylisothiocyanate (TRPA1), others are activated by menthol, camphor, peppermint, etc. Some TRP channels respond to mechanical stimuli like osmotic pressure, volume, stretch, and vibration.

1.4.2 Transient Receptor Potential A1

TRPA1, also referred to as ANKTM1, exhibits several cytoplasmic ankyrin repeats at the *N*-terminus which is a major distinction between TRPA1 and other TRP channels. Transient receptor potential A1 expression was initially demonstrated in dorsal root ganglia, often co-expressed with TRPV1, that responded with a distinct calcium influx after cold stimuli [62, 63, 64]. In 2005, the channel got interest from pharmaceutical companies leading to the development of specific TRPA1 blockers as painkillers. TRPA1 represents a polymodal ion channel as it can be activated by various stimuli, including electrophilic chemicals, oxygen, temperature, and mechanical force [65]. It

was already shown – or at least postulated – that various toxic compounds are able to directly activate TRPA1 channels [50, 66, 67]. Later on, TRPA1 expression in non-neuronal tissues, including skin, lung and digestive organs, was described (Figure 1.6) [52, 59, 64, 68]. However, the biological relevance of TRPA1 in non-neuronal tissue remains unclear.

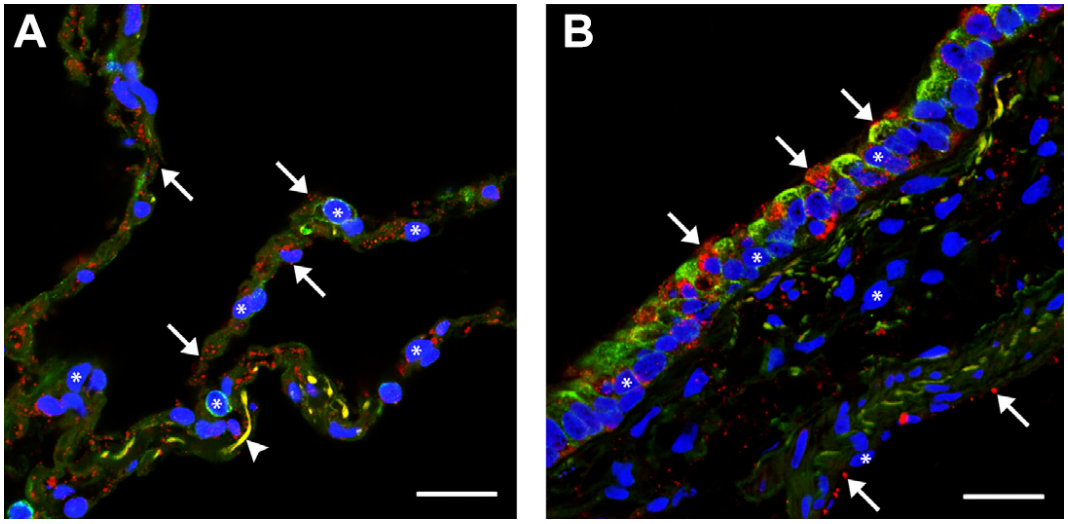

Figure 1.6: TRPA1 expression in human lung tissue. Alveolar (A) and bronchial (B) sections of the human lung were immunostained using a specified anti-TRPA1 antibody. Triple-IHC-stainings (TRPA1: red, arrows; epithelial pan-cytokeratin: green; neuronal βIII tubulin: yellow, arrowheads) revealed a distinct expression of TRPA1 in non-neuronal tissue, as well as in neuronal structures. Especially bronchial epithelium (B) exhibited a pronounced expression of TRPA1 directed towards the lumen. Asterisks indicate DAPI-stained cell nuclei, bar = 20 μm [68].

2 Objectives of the Presented Thesis

Transient Receptor Potential (TRP) ion channels in sensory neurons were shown to respond to a wide range of noxious chemical stimuli, initiating pain, respiratory depression, cough, glandular secretions, and other responses [50]. Especially TRPA1 is activated by a plethora of oxidizing and electrophilic chemicals, most probably by covalent modification of cysteine residues within the ankyrin repeats [50, 66]. SM represents a highly reactive, electrophilic compound that can form adducts with various bio-macromolecules, predominantly at free cysteine residues [69, 70, 71]. Direct activation of TRPA1 channels by SM appears likely but has not been investigated so far.

Thus, the following questions have been addressed and the results are presented in this thesis:

- Do alkylating agents activate TRPA1 channels?
- What are the biological consequences thereof?
- Can TRPA1-blockers prevent SM-induced channel activation?
- Will similar effects be obtained in cells endogenously expressing TRPA1?
- Does SM-induced formation of ROS contribute to TRPA1 activation?

3 Publications

3.1 Activation of the Chemosensing Transient Receptor Potential Channel A1 (TRPA1) by Alkylating Agents

Bernhard Stenger, Franziska Zehfuß, Harald Mückter, Annette Schmidt, Frank Balszuweit, Eva Schäfer, Thomas Büch, Thomas Gudermann, Horst Thiermann, Dirk Steinritz. *Archives of Toxicology* 2015, 89, 1631-1643.

In the first study we investigated whether hTRPA1 channels respond to alkylating agents. To answer this question, a hTRPA1 overexpressing cell line was established and exposed to the monofunctional alkylating compound CEES (2-chloroethylethylsulfide), a frequently used model substance for SM. Initially TRPA1 activation was to be revealed by measuring Ca^{2+}-influx using Fura-2 AM. While the specific TRPA1 activator AITC led to the expected increase of $[Ca^{2+}]_i$, findings after CEES exposure were inexplicable at first glance: CEES affected Fura-2 fluorescence to some degree, however, no concentration-response relationship was observed and signal kinetics were faster than those of the positive control AITC (Supplement Figure 1 A, B, p. 25). Results from further experiments led to the assumption that there is a direct interaction between CEES and Fura-2. As expected, measuring of Fura-2 emission at the isosbestic point (360 nm) – here fluorescence should be independent of Ca^{2+} concentrations – revealed no change for AITC (Supplement Figure 1 C, p. 25). However, in the case of CEES, a significant decrease of fluorescence was evident pointing to a direct interaction between CEES and Fura-2. We concluded that Fura-2 was inappropriate in our experimental setup. Thus, we changed our Ca^{2+}-measurement over to the apoaequorine-assay. Apoaequorine, a protein extracted from the jellyfish *Aquorea victoria* by Shimomura in 1962, changes its conformation upon binding Ca^{2+} in the presence of the substrate coelenterazine, thereby emitting light [72, 73]. Using this setup, no intereference between CEES and apoaequorine was detectable allowing reliable Ca^{2+} measurements. Indeed, our result proved a CEES-induced elevation of $[Ca^{2+}]_i$ through TRPA1 channels (Figure 2, p. 17). Moreover, as TRPA1 was also reported to be activated by protons [74, 75], and H^+ are released during CEES hydrolysis and alkylation reactions, we investigated whether protons were responsible for our results. As expected, pH decreased significantly after having diluted CEES in aqueous media (Supplement Figure 2, p. 26), and some minor channel activation was observed (Figure 3, p. 18). Nevertheless, CEES-induced TRPA1 activation exceeded this effect, thereby demonstrating direct effect of CEES. Remarkably, TRPA1 overexpression was associated with an increased cytotoxicity of CEES that could be counteracted by using specific TRPA1 blockers (Figure 5, p. 19). All findings could be confirmed in A549 lung epithelial cells which endogenously express TRPA1, thereby underlining the biological relevance of the results (Supplement Figure 3 C, p. 27). Thus, a direct link between ion channel activation and enhanced cytotoxicity could be established.

In summary, the key findings of this work were: (i) alkylating compounds activate TRPA1 channels, and (ii) TRPA1 is directly involved in the cytotoxicity of alkylating compounds.

Arch Toxicol (2015) 89:1631–1643
DOI 10.1007/s00204-014-1414-4

ORGAN TOXICITY AND MECHANISMS

Activation of the chemosensing transient receptor potential channel A1 (TRPA1) by alkylating agents

Bernhard Stenger · Franziska Zehfuß · Harald Mückter · Annette Schmidt · Frank Balszuweit · Eva Schäfer · Thomas Büch · Thomas Gudermann · Horst Thiermann · Dirk Steinritz

Received: 1 August 2014 / Accepted: 6 November 2014 / Published online: 14 November 2014

Abstract The transient receptor potential ankyrin 1 (TRPA1) cation channel is expressed in different tissues including skin, lung and neuronal tissue. Recent reports identified TRPA1 as a sensor for noxious substances, implicating a functional role in the molecular toxicology. TRPA1 is activated by various potentially harmful electrophilic substances. The chemical warfare agent sulfur mustard (SM) is a highly reactive alkylating agent that binds to numerous biological targets. Although SM is known for almost 200 years, detailed knowledge about the pathophysiology resulting from exposure is lacking. A specific therapy is not available. In this study, we investigated whether the alkylating agent 2-chloroethyl-ethylsulfide (CEES, a model substance for SM-promoted effects) and SM are able to activate TRPA1 channels. CEES induced a marked increase in the intracellular calcium concentration ($[Ca^{2+}]_i$) in TRPA1-expressing but not in TRPA1-negative cells. The TRP-channel blocker AP18 diminished the CEES-induced calcium influx. HEK293 cells permanently expressing TRPA1 were more sensitive toward cytotoxic effects of CEES compared with wild-type cells. At low CEES concentrations, CEES-induced cytotoxicity was prevented by AP18. Proof-of-concept experiments using SM resulted in a pronounced increase in $[Ca^{2+}]_i$ in HEK293-A1-E cells. Human A549 lung epithelial cells, which express TRPA1 endogenously, reacted with a transient calcium influx in response to CEES exposure. The CEES-dependent calcium response was diminished by AP18. In summary, our results demonstrate that alkylating agents are able to activate TRPA1. Inhibition of TRPA1 counteracted cellular toxicity and could thus represent a feasible approach to mitigate SM-induced cell damage.

Keywords TRPA1 · CEES · Sulfur mustard · Calcium signaling · A549

Abbreviations

AITC	Allyl isothiocyanate
AP18	4-(4-Chlorophenyl)-3-methylbut-3-en-2-oxime
AQ	Distilled water

Electronic supplementary material The online version of this article (doi:10.1007/s00204-014-1414-4) contains supplementary material, which is available to authorized users.

B. Stenger · F. Zehfuß · H. Mückter · T. Gudermann · D. Steinritz
Walther-Straub-Institute of Pharmacology and Toxicology, Ludwig-Maximilian-University Munich, Goethestraße 33, 80336 Munich, Germany

A. Schmidt · F. Balszuweit · H. Thiermann · D. Steinritz (✉)
Bundeswehr Institute of Pharmacology and Toxicology, Neuherbergstraße 11, 80937 Munich, Germany
e-mail: dirk.steinritz@lrz.uni-muenchen.de

A. Schmidt
Department for Molecular and Cellular Sports Medicine, German Sports University Cologne, Am Sportpark Müngersdorf 6, 50933 Cologne, Germany

E. Schäfer · T. Büch
Independent Division of Clinical Pharmacology at Rudolf-Boehm-Institute for Pharmacology and Toxicology, University of Leipzig, Härtelstraße 16-18, 04107 Leipzig, Germany

T. Gudermann
Comprehensive Pneumology Center Munich (CPC-M), German Center for Lung Research, Munich, Germany

T. Gudermann
DZHK (German Centre for Cardiovascular Research), Munich Heart Alliance, Munich, Germany

$[Ca^{2+}]_i$	Intracellular calcium concentration
CEES	2-Chloroethyl-ethylsulfide
DMEM	Dulbecco's modified eagle medium
DMSO	Dimethyl sulfoxide
ECL	Enhanced chemiluminescence
EtOH	Ethanol
FBS	Fetal bovine serum
h	Hours
HEK-A1-E; HEKA1	HEK293 cells, stable transfected with hTRPA1, clone E
HEK-WT; HEKWT	HEK293 wild-type cells
hTRPA1	Human transient receptor potential ankyrin 1
LC_{50}	Lethal concentration, resulting in 50 % decreased cell viability in vitro
mA	Milliampere
mM	Millimolar
µM	Micromolar
min	Minutes
PBS	Phosphate-buffered saline
P/S	Penicillin–streptomycin
RIPA-buffer	Radio-immuno-precipitation-assay buffer
RR	Ruthenium red
s	Seconds
SD	Standard deviation
SDS-PAGE	Sodium dodecyl sulfate polyacrylamide gel electrophoresis
SEM	Standard error of the mean
SM	Sulfur mustard
TIH	Toxic inhalation hazard
TRPA1	Transient receptor potential ankyrin 1
V	Volt
WW	World War

Introduction

Inhalation of noxious chemical substances also known as toxic inhalation hazards (TIHs) causes significant damage to the respiratory system. Toxic lung injury, which is linked to a significant mortality, occurs in severe cases (Büch et al. 2013; Centers for Disease Control and Prevention 2003; Finkelman 2014). Exposure toward TIHs is usually a result of an accidental release of these substances. However, TIHs were also used as chemical warfare agents (e.g., phosgene, sulfur mustard, chlorine) or in terroristic attacks (Dons 2013; McManus and Huebner 2005). The intensive use of TIHs for chemical warfare purposes can be dated back to World War I. However, use of TIHs in armed conflicts has been reported just recently (Hoenig 2002; Thiermann et al. 2013). Sulfur mustard was one of the most frequently used chemical warfare agents in WW I and also later on in the twentieth century (Dons 2013; Rürup et al. 2000; Schmaltz 2005). Despite intense efforts toward chemical disarmament, large stockpiles of this agent still exist. Moreover, SM is comparatively easy to synthesize and thus represents a threat even today (Pechura and Rall 1993; Stewart 2006).

SM is an oily liquid with volatile properties (Centers for Disease Control and Prevention 2003). Reports from WW I revealed that SM can affect a number of organ system including skin, eyes and the respiratory system. The clinical picture of a dermal SM exposure includes erythema, accompanied with almost unbearable pruritus, vesication and wound-healing disorder (Kehe et al. 2009). However, inhalative exposure accounted for almost all fatal cases (Pechura and Rall 1993; Sidell et al. 1997). Similar to skin exposure, sulfur mustard causes vesication of the pulmonary epithelium after inhalation. Due to its poor water solubility, SM is able to reach deep lung compartments (Centers for Disease Control and Prevention 2003; Sidell et al. 1997). Detached epithelium mixes with exsudative fluids, resulting in pseudomembrane formation as a life-threatening event and immediately demands intensive care measures including broncho-alveolar lavage, intubation and PEEP respiration (Ghanei et al. 2011).

Unfortunately, a specific antidote does not exist, and thus, therapy is limited to symptomatic measures (Pohanka 2012; Riccardi 2003; Tewari-Singh et al. 2014). Although sulfur mustard is known for almost 200 years (first synthesis by Depretz in 1822), knowledge about the exact molecular pathology is still limited. The alkylating properties of SM have been intensively investigated: After internal cyclization, one of the chlorine atoms is cleaved off, resulting in the formation of highly reactive intermediates (Kehe et al. 2009). These highly electrophilic intermediates are capable to react with a variety of biological components. Probably, best investigated are the alkylation reactions with nucleic acids (i.e., guanine, adenine), resulting in mono- and bifunctional DNA-adducts (Kehe et al. 2009). In addition, covalent modifications of proteins (e.g., albumin, hemoglobin) have been described (Noort et al. 2008). It is very likely that numerous additional proteins may undergo such modifications.

Recently, it has been reported that oxidizing TIHs such as ozone, acrolein or methylisocyanate can activate chemosensing transient receptor potential (TRP) channels: TRP-channels in sensory neurons were shown to respond to a wide range of noxious chemical stimuli (Bandell et al. 2004; Büch et al. 2013; Jordt et al. 2004; Macpherson et al. 2007; Ramsey et al. 2006), initiating pain, respiratory depression, cough, glandular secretions and other protective responses (Bessac and Jordt 2010; Kinnamon 2012; Ramsey et al. 2006). TRP-channels are regarded to play a pivotal role in the detection of TIHs, in the control of adaptive

responses, and in the initiation of detrimental signaling cascades (Banner et al. 2011; Bessac et al. 2008; Büch et al. 2013). Specifically, TRPA1 is activated by a plethora of electrophilic chemicals, resulting in covalent protein modifications (Bessac and Jordt 2010; Macpherson et al. 2007). In addition to the well-established neuronal expression of TRPA1 (Nilius et al. 2012; Shigetomi et al. 2013), non-neuronal TRPA1 expression (including keratinocytes and lung epithelial cells) is also documented (Büch et al. 2013; Fernandes et al. 2012; Nassini et al. 2012; Schaefer et al. 2013; Simon and Liedtke 2008), suggesting that in these cells TRPA1-mediated effects can occur.

Intermediates of sulfur mustard (e.g., sulfonium/carbenium ion) represent highly electrophilic compounds (Kehe et al. 2009) and thus might directly activate TRPA1 as reported for other reactive compounds (Macpherson et al. 2007). To test this hypothesis, a TRPA1-expressing HEK293 cell line and the alkylating agent 2-chloroethylethylsulfide (CEES) were used. The monoalkylating agent CEES was used as a well-established surrogate for SM (Veress et al. 2010), while proof-of-concept experiments using SM and lung epithelial cells were also conducted. Our results provide first hints that TRPA1 is directly involved in CEES-mediated cytotoxicity.

Materials and methods

Materials

Pure sulfur mustard (purity >99 %, determined by NMR) was purchased from TNO (The Hague, The Netherlands). Minimal essential medium, fetal bovine serum (FBS), phosphate-buffered saline (PBS) and Trypsin–EDTA were obtained from Life Technologies (Gibco, Karlsruhe, Germany). AITC, AP18, CEES and P/S were obtained from Sigma-Aldrich (Steinheim, Germany). AITC is a well-known specific activator of TRPA1 and was used as positive control (Büch et al. 2013). AP18 was shown to specifically block TRPA1 channels (Defalco et al. 2010; Hinman et al. 2006). Cell Proliferation Kit II XTT was purchased from Roche Applied Life Science (Mannheim, Germany). PromoFectin Transfection Reagent was from PromoCell GmbH (Heidelberg, Germany). Coelenterazine was obtained from Biaffin (Kassel, Germany). Ethanol and DMSO were purchased from Carl Roth (Karlsruhe, Germany).

Cell lines

The generation of transfected HEK293 cells (stably expressing TRPA1, further referred to as HEK293-A1-E) has been described previously (Schaefer et al. 2013). HEK293 wild-type (HEK-WT) cells were kindly donated by Vladimir Chubanov, Walther-Straub-Institute, Munich, Germany. Both cell lines were cultured in minimal essential medium, containing L-glutamine and Earle's salts, supplemented with 10 % FBS and 1 % P/S in a humidified atmosphere at 5 % CO_2. A549 cells (CCL-815, LGC Standards GmbH, Germany) with properties of type II alveolar epithelial cells and endogenously expressing TRPA1 were cultured in DMEM containing 10 % FBS and 1 % P/S at a humidified atmosphere at 5 % CO_2 (Büch et al. 2013; Gazdar et al. 1990). All cells were trypsinized for 2 min and resuspended in the respective medium every 2–3 days.

PCR

For PCR analysis of TRPA1 mRNA, a HotStarTaq Plus DNA polymerase was used (Qiagen, Hilden, Germany). PCR was conducted according to the manufacturer's protocol using a BioRad C1000 Touch thermal cycler (BioRad, Heidelberg, Germany). Following an initial activation step at 95 °C for 5 min, 25 cycles were run with 30-s denaturation at 94 °C, 30-s annealing at 56 °C and 1-min elongation at 72 °C. The last step included a final elongation at 72 °C for 10 min to ensure complete DNA strand replication. Primer sequences used for hTRPA1 mRNA detection were designed as Forward 5′-TGTTTCTCAGTGACCACAAT-3′ and Reverse 5′-CTGTGAAGCATGGTCTCATGA-3′ and ordered from Metabion (München, Germany). The PCR product was finally separated in a 1 % agarose electrophoresis (120 V constant for 45 min). DNA was visualized by ethidium bromide staining.

Western blot

For analysis of TRPA1 protein expression, Western blot experiments were performed. For protein isolation, a RIPA-buffer protocol was used. A protease inhibitor (Roche Applied Life Science, Mannheim, Germany) was added to the RIPA-buffer according to the manufacturer's protocol. Cells in a T25 flask were lysed in 0.5 ml RIPA-buffer. Cell lysates were centrifuged at 14,000*g* and 4 °C for 15 min. Supernatants were transferred to a new vial. 15–30 µg whole cell extracts were loaded on a 10 % polyacrylamide gel. SDS-PAGE was run at constant 100 mA using a Bio Rad Mini-PROTEAN Tetra Cell chamber (Bio-Rad, Heidelberg, Germany). After 1D separation, proteins were transferred to a 0.2-µm nitrocellulose membrane using a Bio Rad Mini Trans-Blot Cell (Bio-Rad, Heidelberg, Germany). Wet-Blotting was conducted with constant 125 V for 1 h. Blocking was done by 5 % skimmed milk powder and 0.1 % Tween 20 dissolved in PBS. As primary antibody, a rabbit polyclonal antihuman TRPA1 antibody (PAB 11992, Abnova, Taipei City, Taiwan) at 2 µg/ml concentration was used. Detection was done by a goat anti-rabbit

peroxidase antibody (1706515, BioRad, Heidelberg, Germany) diluted 1:7,500 and subsequent enhanced chemiluminescence detection (ECL).

Functional measurement of Ca^{2+} influx using Fura-2 AM

Activation of TRPA1 was initially explored by measuring intracellular Ca^{2+}-influx using Fura-2 AM ester as described earlier (Almers and Neher 1985). In brief, cells were harvested using 0.05 % EDTA-Trypsin, loaded with 1 µM Fura-2 AM and incubated at room temperature for 30 min. Afterward, cells were washed once with MEM. Subsequently, 1.2×10^6 cells/ml were transferred into a Greiner 96-well flat microplate (Greiner Bio-One, Frickenhausen, Germany). Changes in Fura-2 AM fluorescence were detected using a Tecan infinite m200Pro plate reader (equipped with a gas control module to maintain 37 °C and 5 % CO_2 within the plate reader). To ensure homogenous cell suspension, a 30-s orbital shake with 5-mm amplitude was implemented before each measurement. Fluorescence emission was detected at 510 nm according to the manufacturer's protocol. Excitation wavelength was adjusted to 340 nm for detecting high calcium concentrations, to 360 nm where Fura-2 AM is insensitive to calcium (isosbestic point) and to 380 nm to detect low calcium concentrations, respectively. Fluorescence was recorded over time and CEES (10,000–3,333–123 µM), HCl (1,000 µM) or AITC (15 µM) were injected. The ratio of 340 and 380 nm was calculated to assess changes in the intracellular calcium concentration.

Transient transfection of Ca^{2+}-sensitive aequorin plasmid

The aequorin-coding plasmid was kindly provided by Andreas Breit, Walther-Straub-Institute Munich, Germany. 10 µg of the DNA-construct was diluted in 500 µl MEM without any additional supplements. 12 µl PromoFectin were diluted in 500 µl MEM without any further supplements. Both solutions were thoroughly mixed by vortexing and incubated for 30 min at room temperature. The DNA-PromoFectin solution was then transferred into a T25 cell culture flask before 4 ml of cell suspension containing a total of 5×10^6 cells were seeded on top. Cells were cultured for up to 4 days.

Functional measurement of Ca^{2+} influx using an aequorin assay

Activation of TRPA1 primarily results in a calcium influx. Thus, we measured changes in intracellular calcium concentrations using the calcium-sensitive photoprotein aequorin as described earlier (Kendall and Badminton 1998; Shimomura et al. 1974). Prior to the measurement, aequorin-transfected cells were loaded with 5 µM of the apoaequorin chromophore coelenterazine for 15 min at 37 °C and a humidified atmosphere with 5 % CO_2. Afterward, cells were washed with PBS once, harvested with trypsin, and transferred to 5 ml MEM without phenol red, but containing 10 % FCS and 1 % P/S. Cell suspensions were centrifuged at 500*g* for 5 min. The supernatants were removed. Cell pellets were resuspended to a concentration of 1.2×10^6 cells/ml in MEM (without phenol red and without any additional supplements). 200 µl of the cell suspension were transferred to a Greiner 96-well Lumitrac 200 Plate (Greiner Bio-One, Frickenhausen, Germany). Measurements were performed using a Tecan infinite m200Pro plate reader (equipped with a gas control module to maintain 37 °C and 5 % CO_2 within the plate reader). To ensure homogenous cell suspension, a 30-s orbital shake step (amplitude of 5 mm) was performed before each measurement. Luminescence was recorded with an integration time of 1,000 ms over at least 2 min. 10 µl injections of the respective chemicals [CEES, SM, AITC (positive control) or EtOH (solvent control)] was done after 20-s baseline recording. To avoid rapid hydrolysis of CEES and SM, both chemicals were first dissolved in EtOH at a concentration of 400 mM. Solutions were then adjusted to the 20-fold of the concentration intended for exposure. Immediately before the measurements, 10 µl CEES- or SM-solution was injected into the well containing 190 µl MEM without phenol red. CEES or SM was thereby diluted by the factor 20 to the intended final concentration (CEES 30,000–500 µM; SM 500 µM). The TRP-channel inhibitor AP18 was injected 15 s before exposure as described earlier (Nakatsuka et al. 2013). Normalization was done by dividing raw values by the mean of the baseline values, resulting in a relative increase in luminescence normalized to baseline levels.

Determination of pH changes by CEES hydrolysis in MEM or distilled water

During CEES hydrolysis, equimolar amounts of protons are generated. To assess their influence on pH values, 10 mM CEES were added to either MEM (supplemented with 10 % FCS) or to distilled water, respectively. pH values were determined prior to CEES addition, immediately after and after 30 or 60 min using a WTW inolab ph7310 pH meter (WTW, Weilheim, Germany).

Cell viability assay XTT

CEES toxicity was assessed by using a XTT cell viability assay. Cells were seeded at a density of 4×10^4 cells per well (96-well format) for HEK293 cells in a total of 75 µl MEM (containing phenol red, 10 % FBS and 1 % P/S). Cells were grown to approximately 90 % confluence for 24 h. After 24 h, cells were exposed to CEES in different concentrations. To avoid rapid hydrolysis, CEES was first

dissolved in 100 % EtOH. Afterward, a dilution (2× final concentration) in MEM (containing phenol red, 10 % FBS and 1 % P/S) was done just before exposure. 75 µl of this CEES solution was pipetted on top of the seeded cells, resulting in a total of 150 µl medium (1:2 dilution), containing the defined final concentration of CEES per well. Final concentrations of CEES ranged from 10,000 to 0.508 µM. EtOH (0.125 %) was used as solvent control. Cell viability was measured after 24 h without a prior medium change. Following the manufacturer's protocol, 75 µl of XTT reagent was pipetted on top of the cells and the plate was incubated for 60 min (humidified atmosphere, 37 °C and 5 % CO_2). Absorption was measured at a wavelength of 450 nm and 650 nm (reference) using a Tecan infinite m200Pro plate reader.

Statistics

Statistical analysis was processed using GraphPad prism v6.0 software. For statistical comparison of the maximal response, one-way ANOVA with Tukey correction for multiple comparisons was performed. p values <0.05 were regarded significant.

Results

Expression of TRPA1 in HEK293-A1-E cells

Expression of functional TRPA1 in HEK293-A1-E cells was confirmed by PCR, Western blot analysis and AITC-induced calcium influx. Both PCR and Western blot analysis revealed a distinct positive signal for TRPA1 mRNA (Fig. 1a) or TRPA1 protein expression (Fig. 1b). As expected, WT cells did not show TRPA1 mRNA or protein expression (Fig. 1a, b). 15 µM AITC (positive control) initiated a pronounced transient of the intracellular calcium concentration ($[Ca^{2+}]_i$) in HEK293-A1 cells with a slow decay over a period of about 90 s, while HEK293-WT cells did not show an AITC-induced change in $[Ca^{2+}]_i$ (Fig. 1c). EtOH (0.5 % v/v, solvent control) did not affect $[Ca^{2+}]_i$ in HEK293-A1-E or HEK293-WT cells (Fig. 1c).

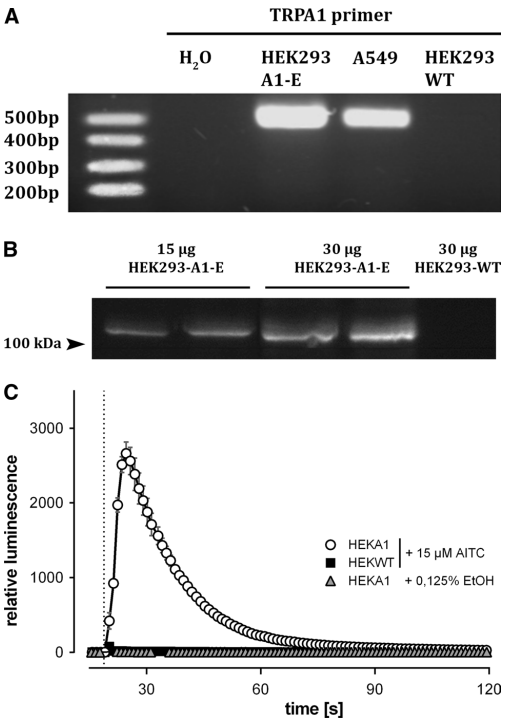

Fig. 1 **a** Representative PCR detection of hTRPA1 mRNA expression in HEK293-WT, transfected HEK293-A1-E and basal expression in A549 cells. HEK293-WT cells did not show hTRPA1 mRNA expression, whereas the other investigated cell types revealed a distinct expression of hTRPA1 mRNA. HEK293-A1-E showed higher levels of hTRPA1 mRNA expression compared with A549 cells. **b** Representative Western blot analysis of HEK293-A1-E and HEK293-WT cell lysates using antihuman TRPA1 antibody. Two different total protein amounts (15 and 30 µg) were analyzed for transfected HEK293-A1-E, and 30 µg of total protein were analyzed for HEK293-WT cells. In accordance with the manufacturer's information, the antibody detects a specific protein slightly above 100 kDa. WT cells did not show a specific band, whereas HEK293-A1-E cells did show a distinct protein band. **c** HEK293-A1-E (*white circles, gray triangles*) as well as HEK293-WT cells (*black squares*) were transfected with aequorin and stimulated with 15 µM AITC (*circles, squares*) or to ethanol (EtOH) (*triangles*) as solvent control. The *vertical dotted line* indicates the time of injection. HEK293-A1-E cells responded with a distinct increase in aequorin luminescence, indicating a calcium influx. HEK293-WT cells did not show a specific response. EtOH stimulation of HEK293-A1-E cells did not evoke a specific signal. All experiments were conducted with $n = 3$. Mean values ± SEM are given

Fura-2 AM is inappropriate to detect CEES-induced increase in $[Ca^{2+}]_i$

Fura-2 AM is as a sensitive indicator dye for measuring changes in intracellular calcium concentrations. As expected, AITC led to a distinct increase in intracellular calcium in Fura-2 AM experiments (Suppl. Figure 1A). However, we have not been able to detect a reliable increase in Fura-2 AM fluorescence after exposure of HEK293-A1-E cells to CEES. Interestingly, there was a very small increase in fluorescence immediately after CEES exposure. However, the Fura-2 AM signal did not increase over time and occurred faster compared with the positive control AITC (Suppl. Figure 1A, B). Moreover, no obvious CEES concentration dependency was observed. Fluorescence at

the isosbestic point (360 nm) was decreased even after low CEES exposures, indicating a direct interaction between Fura-2 AM and CEES (Suppl. Figure 1C). HCl (i.e., released during CEES hydrolysis) did not affect Fura-2 AM fluorescence at the isosbestic point (Suppl. Figure 1C).

CEES-induced calcium influx in HEK293-A1-E compared with HEK293 WT

Exposure of HEK293-A1-E cells to CEES resulted in a distinct increase in the intracellular calcium concentration ($[Ca^{2+}]_i$) as determined by aequorin luminescence (Fig. 2a). Exposure of HEK293-WT cells to CEES or exposure of HEK293-A1-E to EtOH (solvent control) did not affect $[Ca^{2+}]_i$.

The CEES-induced calcium response in HEK293-A1-E cells followed a concentration–response relationship with an EC_{50} value of 7,392 µM when comparing relative amplitudes elicited by different CEES concentrations (Fig. 2b).

Proton release during CEES hydrolysis

Protons (i.e., H_3O^+, further referred to as protons) are generated by the rapid hydrolysis of CEES in aqueous media. Notably, stimulation of human TRPA1 by protons has been described (de la Roche et al. 2013; Wang et al. 2011) and could contribute to CEES-induced effects on this channel. To assess the influence of these protons on TRPA1 activation, we determined the acidification during CEES hydrolysis in MEM and PCR-grade AQ using a pH meter (Suppl. Figure 2). As expected, in distilled water, an instantaneous acidification was detectable. In MEM, only a minor acidification was determined most probably due to the buffering capacity of the cell culture medium. The decrease in pH was highly significant in both groups (MEM and AQ). However, despite the statistical significance, initially only minor acidification (Δ pH 0.246) in MEM occurred.

Influence of protons on TRPA1 activation and proton effect corrected CEES-induced TRPA1 activation

Although only marginal CEES-induced pH changes were detectable in MEM, we investigated whether protons derived from CEES hydrolysis had any effect on TRPA1 activation as measured by aequorin luminescence. We exposed HEK293-A1-E cells to different HCl concentrations corresponding to the proton concentration generated by a complete hydrolysis of the respective CEES concentration. Injection of HCl indeed activated TRPA1 channels to a minor extent (Fig. 3a), in line with recent findings about proton-sensing properties of TRPA1 (de la Roche et al. 2013; Wang et al. 2011). To differentiate between TRPA1 activation by protons derived from CEES hydrolysis or

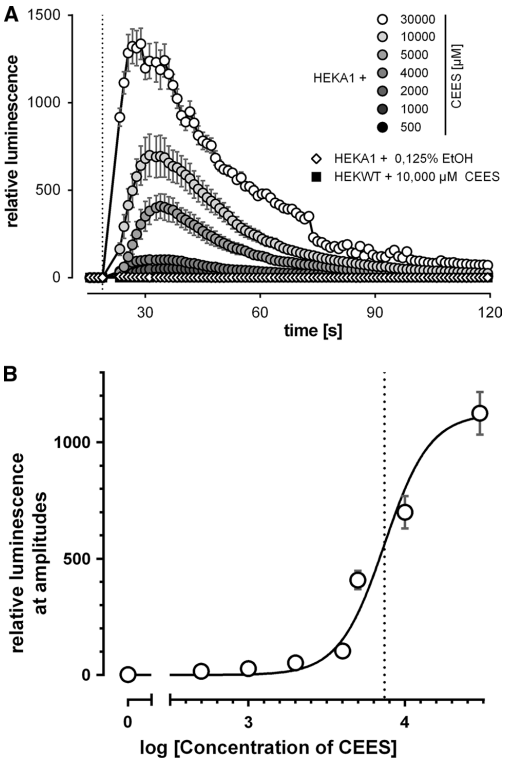

Fig. 2 **a** HEK293-A1-E (*circles*) and HEK293-WT (*black squares*) were exposed to CEES, and $[Ca^{2+}]_i$ was determined by aequorin luminescence. The *vertical dotted line* indicates the CEES injection. HEK293-A1-E showed a distinct calcium influx after CEES exposure following a concentration–response relationship. Ethanol (solvent control, *diamonds*) injections had no effect in HEK293-A1-E cells. HEK293-WT cells did not respond to CEES injections. Data points from HEK293-WT cells disappear behind the solvent control data. All experiments were conducted with $n = 3$. Mean values ± SEM are given. **b** Concentration–response relationship displaying peak luminescence values (shown in **a**). The CEES-induced calcium response in HEK293-A1-E cells followed a concentration–response relationship with an EC_{50} value of 7,392 µM (*dotted line*). All experiments were conducted with $n = 3$. Mean values ± SEM are given

by CEES itself, we performed additional experiments that allowed a direct comparison of these effects (experiments were performed with batches of cells derived from the same transfection procedure). Our results clearly demonstrate a distinct increase in $[Ca^{2+}]_i$ after CEES exposure that exceeds proton-induced TRPA1 activation and thus can be specifically attributed to CEES (Fig. 3b–d). The kinetics of the respective Ca^{2+} transients also differed: CEES exposures resulted in a significantly longer transient compared with proton-induced TRPA1 activation.

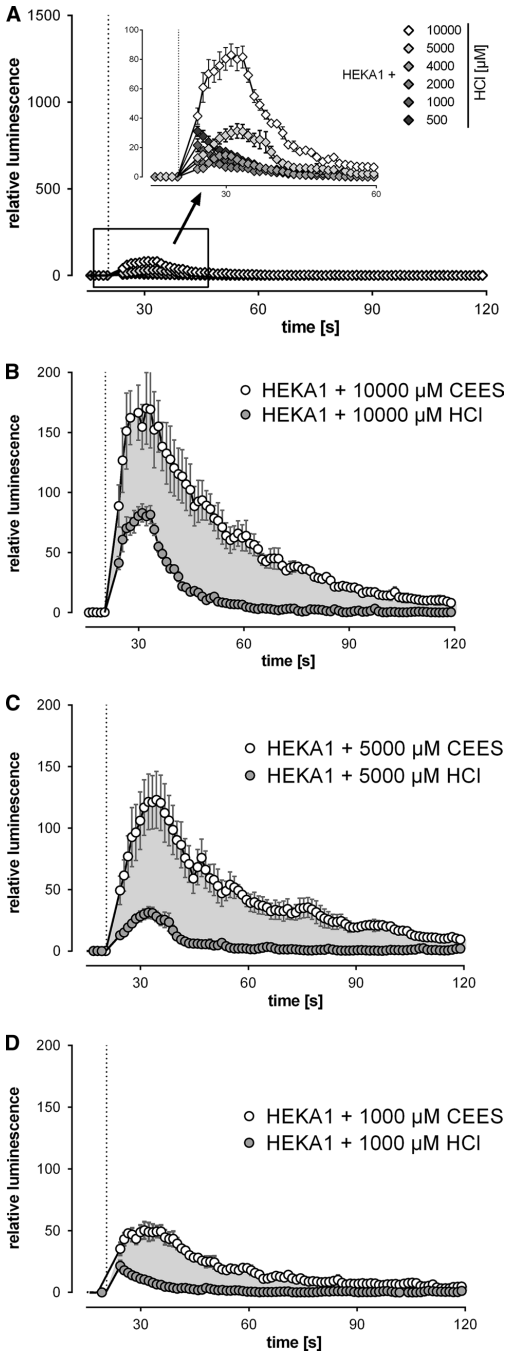

Fig. 3 Hydrolysis of CEES in aqueous solutions results in the formation of protons and highly reactive intermediates. **a** The influence of protons on TRPA1 activation was assessed by the exposure of HEK293-A1-E cells to HCl in increasing concentrations (500–10,000 µM HCl) and detection of aequorin luminescence. Although the increase in pH in MEM after HCl injection was only minor (Suppl. Figure 2), a distinct but small proton-induced increase in $[Ca^{2+}]_i$ was detectable that followed a concentration–response relationship. The *insert* represents a zoom of the relevant data. All experiments were conducted with $n = 3$. Mean values ± SEM are given. **b–d** Increase in $[Ca^{2+}]_i$ over time determined by aequorin luminescence, following injections of defined concentrations of CEES or corresponding HCl concentrations. A distinct increase in $[Ca^{2+}]_i$ after CEES exposure that exceeded the proton-induced TRPA1 activation was observed, which is indicated with the gray areas between the curves. All experiments were conducted with $n = 3$. Mean values ± SEM are given

Effect of the TRP-channel blocker AP18 on CEES-induced calcium influx in HEK293-A1-E cells

As CEES was shown to activate TRPA1-channels, we next investigated whether a TRP-channel blocker was able to prevent CEES-induced calcium responses. HEK293-A1-E cells were pre-incubated with AP18 and exposed to 7,500 µM CEES, closely approximating the EC_{50} determined before, and changes in $[Ca^{2+}]_i$ were determined by aequorin luminescence. HEK293-A1-E cells without AP18 pre-incubation were used as controls. Negative controls were conducted by pre-incubation of HEK293-A1-E with AP18 followed by injection of 5 % EtOH.

We observed a reduction of CEES-induced calcium influx in the presence of AP18 compared with non-pre-incubated cells (Fig. 4a). Blocking of TRPA1 by AP18 and the decrease in calcium influx followed a concentration–response relationship (Fig. 4b). The IC_{50} was determined at 0.62 µM AP18.

CEES toxicity in HEK293-A1-E and HEK293-WT cells

Effects of CEES on cell viability were measured using the XTT assay. HEK293-A1-E and HEK293-WT cells were exposed to different concentrations of CEES. Cell viability was assessed 24-h post-exposure. HEK293-A1-E cells were more sensitive to the alkylating agent with a calculated LC_{50} value of 380 µM compared with a LC_{50} of 904 µM in WT cells (Fig. 5). The 95 % confidence intervals did not overlap, indicating a significant difference between the two investigated cell lines with regard to CEES toxicity.

Influence of the TRP-channel blocker AP18 on CEES-induced cytotoxicity

Pre-incubation of HEK293-A1-E cells with 50 µM AP18 diminished CEES-induced cytotoxicity 24-h post-exposure,

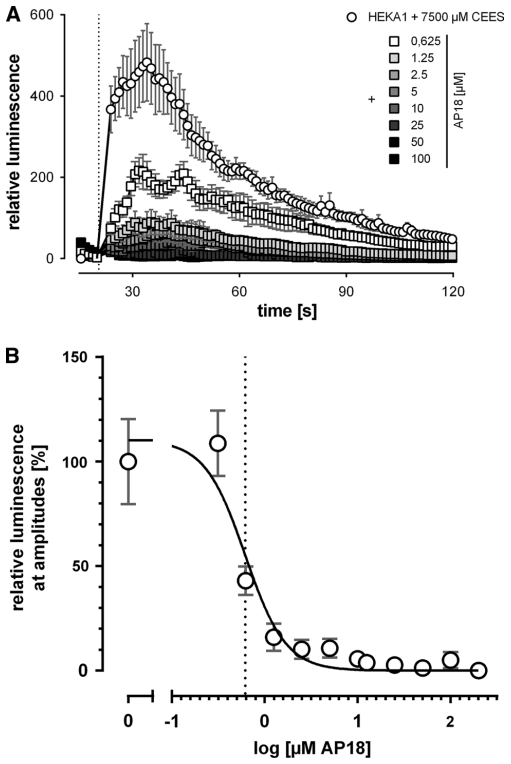

Fig. 4 **a** HEK293-A1-E cells were pre-incubated with different concentrations AP18 and exposed to 7,500 µM CEES, closely approximating the EC_{50}. The *vertical dotted line* indicates the CEES injection. AP18 was able to prevent the CEES-induced calcium influx measured by aequorin luminescence in a concentration-dependent manner. **b** Concentration–response relationship displaying peak luminescence values (shown in **a**) determined 0.62 µM AP18 as IC_{50} (*dotted line*) with regard to CEES-induced TRPA1 activation. All experiments were conducted with $n = 3$. Mean values ± SEM are given

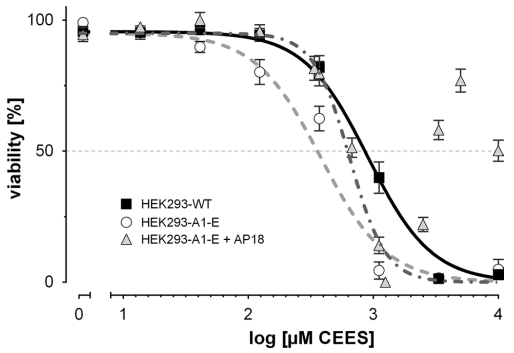

Fig. 5 Cell viability of HEK293-A1-E (*white circles, triangles*) and HEK293-WT (*black squares*) cells after exposure to CEES was assessed 1d post-exposure by XTT assays according to the manufacturer's protocol. HEK293-A1-E cells were found more sensitive toward CEES (LC_{50} 380 µM, *dashed line*). HEK293-WT cells were found more resistant toward CEES exposure (LC_{50} 904 µM, *solid line*). Pre-incubation of HEK293-A1-E cells with AP18 (*upward triangles*) diminished cytotoxicity (LC_{50} 646 µM, *dashed/dotted line*) up to a CEES concentration of 675 µM. CEES concentrations of 1,111 µM resulted in a complete loss of cell viability also in the presence of AP18. XTT responses suggesting strong metabolic activity after CEES exposure of 3,333 µM and above in the presence of AP18 had to be considered erratic and were not taken into account for curve fitting. All experiments were conducted with at least $n = 3$. Mean values ± SEM are given

especially at CEES concentrations up to 675 µM (Fig. 5). Within that range, cell viability (measured by XTT assay) resembled that of HEK293-WT cells, demonstrating protective properties of AP18. At higher CEES concentrations, results were inconsistent, although reproducible. Interference of AP18 with the XTT assay was intensively checked but was not found. CEES concentrations of 1,111 µM resulted in a complete loss of cell viability also in the presence of AP18. XTT responses suggesting strong metabolic activity after CEES exposure of 3,333 µM and above in the presence of AP18 had to be considered erratic and were not taken into account for curve fitting. The parameters of the fitting curve (i.e., range, bottom) were adjusted accordingly. The LC_{50} was then determined at 646 µM CEES, which is clearly different from the LC_{50} of 380 µM in HEK293-A1-E cells. Confidence intervals of the LC_{50} in HEK293-A1-E cells with or without AP18 pre-treatment did not overlap, indicating a significant benefit of AP18 regarding CEES toxicity in HEK293-A1-E cells.

Calcium influx in HEK293-A1-E cells after SM exposure

So far, we investigated the effect of CEES, which represents a model substance for the chemical warfare agent sulfur mustard on TRPA1 activation. In a proof-of-concept experiment, HEK293-A1-E cells were exposed to 500 µM SM in order to evaluate whether SM had similar effects on TRPA1. After SM exposure, a rapid and distinct increase in calcium influx determined by aequorin luminescence was observed in HEK293-A1-E cells (Fig. 6), underlining the results obtained after CEES exposure. WT cells which did not respond to CEES exhibited a weak increase in $[Ca^{2+}]_i$ after exposure to 500 µM SM.

Calcium influx in A549 lung epithelial cells after CEES exposure and effects of the TRP-channel blocker AP18

HEK293-A1-E cells overexpressing TRPA1 channels were used to study the effects of alkylating agents on TRPA1

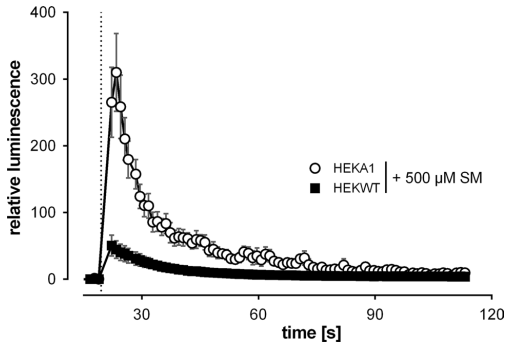

Fig. 6 HEK293-A1-E (*white circles*) or HEK293-WT cells (*black squares*) were exposed to 500 µM SM. The *vertical dotted line* indicates the SM injection. HEK293-A1-E cells revealed a distinct increase in $[Ca^{2+}]_i$ calcium influx after SM exposure as measured by aequorin luminescence. WT cells showed some minor effects. All experiments were conducted with $n = 3$. Mean values ± SEM are given

in general. A549 cells (an established human lung epithelial cell line endogenously expressing TRPA1 (Büch et al. 2013; Mukhopadhyay et al. 2011) were used for additional experiments in order to investigate the effect of alkylating agents on lung epithelial cells. A549 cells were transfected with aequorin and exposed to 2,500 µM CEES. A small but distinct increase in relative aequorin luminescence was detectable, providing evidence that TRPA1-expressing lung epithelial cells respond to alkylating agents with a calcium influx (Suppl. Figure 3A). As expected, the maximum response was lower compared with HEK293-A1-E cells that overexpress TRPA1. Pre-incubation of A549 with AP18 followed by a 2,500 µM CEES exposure resulted in a significant decrease in CEES-induced calcium influx that followed a concentration–response relationship (Suppl. Figure 3B, C). However, a complete inhibition of calcium influx could not be achieved.

Discussion

TRP-channels are supposed to function as sensors for toxic chemicals (Bessac et al. 2008). It has been postulated that TRPA1 is activated by electrophilic substances, but up to now, it has not been investigated whether alkylating substances including CEES and SM are able to activate TRPA1. Therefore, we investigated the effect of CEES and SM on TRPA1 channels.

Initially, we used Fura-2 AM to detect changes in $[Ca^{2+}]_i$. AITC which is a well-established activator of TRPA1 led to a distinct increase in intracellular calcium in Fura-2 AM experiments, as expected. However, results from CEES exposure experiments were inconsistent. We assumed that the Fura-2 AM results might be incorrect and misleading. A closer look at the results revealed that the fluorescence at the isosbestic point (360 nm) was decreased even after low CEES exposures, indicating a direct interaction between Fura-2 AM and CEES. This hypothesis was supported by the finding that HCl (i.e., released during CEES hydrolysis) did not affect Fura-2 AM fluorescence at the isosbestic point. As a conclusion, Fura-2 AM measurements in the presence of alkylating substances are flawed and inappropriate. Therefore, we changed to aequorin-based calcium measurements, which were not influenced by alkylating agents.

Using aequorin-based calcium measurements, we were able to demonstrate that the alkylating agent CEES increased intracellular calcium in TRPA1-overexpressing cells in a concentration-dependent manner. The EC_{50} was determined at approximately 7,500 µM CEES, which at a first glance indicates a low affinity of CEES toward TRPA1. However, it is important to note that the nominal concentration of CEES in the medium is not necessarily identical with the CEES concentration present at TRPA1-channels: Hydrolysis of CEES will immediately occur after injection of CEES into aqueous solutions, thus decreasing the amount of CEES. Moreover, CEES is known to interact with macromolecules (e.g., albumin), which are present in the medium, thus decreasing the amount of unbound CEES even more. As hydrolysis and covalent interactions of CEES with other proteins cannot be prevented, the EC_{50} determined in our experiments might be over-estimated to some extent. However, pre-incubation with the TRP-channel inhibitor AP18 was able to diminish or even prevent the CEES-induced calcium influx, indicating a direct activation of TRPA1 by CEES.

Overexpression of TRPA1 in HEK293-A1-E cells aggravated CEES toxicity compared with HEK293-WT cells. Pre-incubation with AP18 showed distinct protective effects in the lower dosage range of CEES exposure. At higher CEES concentrations, AP18 was unable to counteract CEES-induced cytotoxicity. This is in line with results described by Sawyer et al. who postulated that perturbations of $[Ca^{2+}]_i$ do not play a major role in SM-induced cytotoxicity in keratinocytes (Sawyer and Hamilton 2000). DNA alkylation is predominantly responsible for cytotoxicity at high CEES concentrations. It is unlikely that inhibition of ion channels (e.g., TRP-channels) can have an effect in the means of preventing DNA alkylation and thus preventing cell death. This hypothesis can explain our results at high CEES concentrations. However, after exposure to low concentrations of CEES (when DNA alkylation is reversible), a distinct protective effect was obvious, indicating that additional pathways are involved in mediating CEES cytotoxicity. Thus, our results provide reliable hints

that TRP-channels are directly involved in the molecular toxicology.

SM exposure led to a more pronounced increase in $[Ca^{2+}]_i$ compared with CEES exposures. As known from other studies, CEES is less toxic than SM (Gautam et al. 2006). Thus, a higher calcium influx after SM and the weaker response to CEES exposure are in line with those results. With regard to the chemical structure, we speculate that SM as a bifunctional alkylating agent shows a higher alkylation activity than the monofunctional CEES. Nevertheless, both agents induced a distinct calcium influx with a maximum relative response at a comparable time after exposure, indicating that alkylating agents as substance class are able to activate TRPA1 channels.

Compared with AITC-induced TRPA1 activation, the calcium influx induced by alkylating agents reached peak intensity within a similar time when either high CEES concentrations (30,000 µM) or SM were used. However, the absolute peak intensity induced by AITC was not reached by CEES or SM in our experiments. CEES concentrations of 10,000 µM and below also activated TRPA1, but effect was both weaker and slower, i.e., requiring more time to reach its peak intensity. The aequorin luminescence signal declined within approximately 60 s after AITC and SM-induced TRPA1 activation, but could be detected for approximately 90 s after CEES exposure.

It was demonstrated that AITC activates TRPA1 through a mechanism involving direct covalent (but reversible) modification of specific intracellular cysteine residues within the channel protein (Hinman et al. 2006). Moreover, it was discussed that TRPA1 activation through various agonists relied on the agonists' reactivity. The calcium influx through irreversible TRPA1 modification was shown as long lasting and could be blocked by the TRP-channel inhibitors (Hinman et al. 2006). CEES- and SM-induced protein modifications are considered as highly stable. An irreversible modification of TRPA1 is therefore most likely to occur, although it has not been demonstrated yet. Our aequorin-based experiment revealed an immediate increase in luminescence after CEES/SM exposure. The signal declined within minutes to basal levels, which is at a glance not in line with the findings of Himan et al. (2006) that suggested a long-lasting TRPA1 activation after irreversible modifications. However, it has to be noted that this was found with Fura-2 AM-based calcium measurements that turned out inappropriate in our particular experimental settings. Remarkably, also the AITC-induced luminescence signal differed significantly from that in Fura-2 AM-based experiments (Fig. 1c and Fig. Suppl. 3A). It can be speculated that aequorin-based calcium measurements indicate changes in calcium fluxes in first line rather than providing stable signals at constant calcium fluxes. At the moment, we cannot give a definite answer whether CEES/SM causes irreversible modifications of TRPA1 and causes a long-lasting calcium influx.

TRPA1 was found to be sensitive for protons (de la Roche et al. 2013). During hydrolysis of CEES (and also SM), a stoichiometric quantity of protons is generated in equimolar concentrations (with regard to SM in a twofold quantity). We investigated the effect of these protons on TRPA1 activation. Indeed, HCl exposure activated TRPA1, resulting in a minor but distinct increase in intracellular calcium. However, this effect was of short duration. CEES exposure resulted in a significant additional increase in calcium, underlining a direct interaction of CEES and TRPA1.

Neuronal TRPA1 expression is well established (Nilius et al. 2012; Shigetomi et al. 2013). Recently, non-neuronal TRPA1 expression including keratinocytes and lung epithelial cells was described (Büch et al. 2013; Fernandes et al. 2012; Nassini et al. 2012; Simon and Liedtke 2008). The A549 human lung epithelial cell line is one example for an endogenous, non-neuronal expression of TRPA1 (Büch et al. 2013; Mukhopadhyay et al. 2011). A549 responded with a calcium influx after AITC stimulation that could be inhibited by the TRP-channel blocker RR (Büch et al. 2013). It is feasible that TRPA1 functions as a chemosensing receptor in these cells. Therefore, we investigated whether the results obtained in our model cell line were transferable to lung epithelial cells. In line with our results so far, CEES exposure of A549 cells resulted in a significant calcium influx. However, the response was weaker compared with HEK293-A1-E cells. This was expected as A549 cells do not overexpress TRPA1 but express TRPA1 endogenously. AP18 diminished the CEES-induced calcium influx, but in contrast to HEK293-A1-E cells, the calcium influx could not be completely prevented. AP18 was shown to block TRPA1 with a high affinity, whereas other TRP-channels were not or only partially blocked (Petrus et al. 2007). It can be speculated that in A549 cells, additional calcium-gating channels are involved in the CEES-induced calcium influx.

Patients that have been exposed to sulfur mustard report an almost unbearable pruritus that does not respond to antihistamines. TRPA1 was shown to be required for histamine-independent itch. TPRA1-deficient mice displayed almost no scratching when exposed to pruritogens that act independently of histamine (Wilson et al. 2011). Therefore, blocking of TRPA1 channels is a highly promising approach to treat this specific aspect of SM poisoning.

In summary (Fig. 7), we have demonstrated for the first time that TRPA1 is directly activated by alkylating agents (CEES and SM). Protons that are generated during CEES hydrolysis also contribute to TRPA1 activation, but CEES does have significant additional effects. The exact mechanism, by which CEES or CEES intermediates provoke the activation of TRPA1 channels, will be examined in further

Arch Toxicol (2015) 89:1631–1643 1641

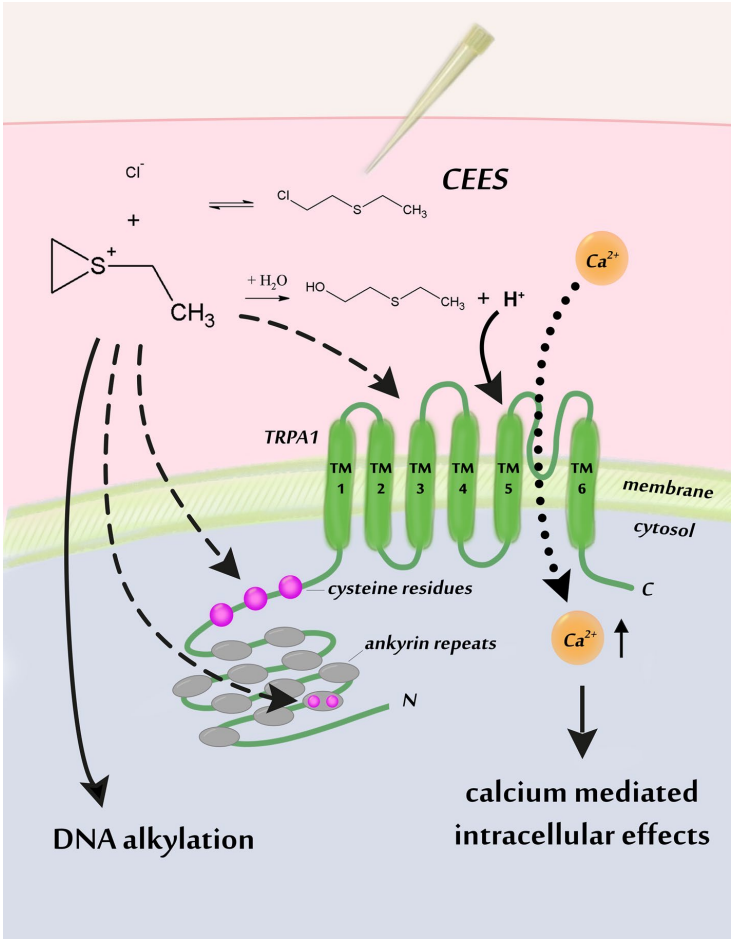

Fig. 7 Potential mechanisms of CEES-induced and TRPA1-mediated calcium influx. Intracellular cysteine residues have been discussed as targets for covalent modifications, including alkylation, resulting in TRPA1 activation. Alkylating properties of CEES with regard to DNA and proteins are well known. Thus, alkylation of nucleophilic amino acid residues, including intracellular cysteine residues of TRPA1, is likely to occur. Proton-induced activation of TRPA1, associated with the transmembrane domains 5 and 6, has also been discussed. Thus, proton release during CEES hydrolysis may contribute to a direct TRPA1-mediated calcium influx. However, the calcium influx induced by CEES is more intense and sustained than the HCl induced increase in $[Ca^{2+}]_i$. Thus, our experiments revealed a distinct TRPA1 activation that can be attributed solely to CEES

studies. As shown in Fig. 7, it is plausible that covalent modifications of cysteine residues by reactive intermediates could be responsible for the observed activation of TRPA1. This has been described for other reactive chemicals (Macpherson et al. 2007), but has to be proven for alkylating substances. Whether targets other than cysteine residues are covalently modified is currently unknown and will be investigated in future studies. Moreover, non-covalent TRPA1 modifications are also possible and have to be taken into account. Again, this has to be explored in future studies.

TRPA1 overexpression led to an increase in CEES toxicity. The TRPA1-channel blocker AP18 diminished or even prevented the CEES-induced and TRPA1-mediated calcium influx. A protective effect of AP18 with regard to CEES toxicity could be found at lower CEES concentrations. A549 lung epithelial cells, endogenously expressing TRPA1, revealed a distinct CEES-induced calcium influx that could be diminished by AP18.

Future studies will be conducted to assess whether CEES and other alkylating agents covalently modify TRPA1 at thiol moieties of cysteine amino acid residues and thus activate TRPA1 or if other binding sites of TRPA1 are required for the activation by alkylating agents. Moreover, the biological effects of alkylating agents-induced TRPA1 activation have to be investigated. Regulation of cell death, inflammation, pain and pruritus might be promising subjects for further studies.

Acknowledgments We thank Vladimir Chubanov, Andreas Breit and Ram Prasad for their helpful support. This research was supported by the Transregional Collaborative Research Center 152, Project P15 and by a contract (E/UR2 W/CF504/CF560) of the German Armed Forces.

Conflict of interest The authors declare no conflict of interest.

References

Almers W, Neher E (1985) The Ca signal from fura-2 loaded mast cells depends strongly on the method of dye-loading. FEBS Lett 192(1):13–18. doi:10.1016/0014-5793(85)80033-8

Bandell M, Story GM, Hwang SW, Viswanath V, Eid SR, Petrus MJ, Earley TJ, Patapoutian A (2004) Noxious cold ion channel TRPA1 is activated by pungent compounds and bradykinin. Neuron 41(6):849–857. doi:10.1016/S0896-6273(04)00150-3

Banner KH, Igney F, Poll C (2011) TRP channels: emerging targets for respiratory disease. Pharmacol Ther 130(3):371–384. doi:10.1016/j.pharmthera.2011.03.005

Bessac BF, Jordt S (2010) Sensory detection and responses to toxic gases: mechanisms, health effects, and countermeasures. Proc Am Thorac Soc 7(4):269–277. doi:10.1513/pats.201001-004SM

Bessac BF, Sivula M, von Hehn CA, Escalera J, Cohn L, Jordt S (2008) TRPA1 is a major oxidant sensor in murine airway sensory neurons. J Clin Investig 118(5):1899–1910. doi:10.1172/JCI34192

Büch TR, Schäfer EA, Demmel M, Boekhoff I, Thiermann H, Gudermann T, Steinritz D, Schmidt A (2013) Functional expression of the transient receptor potential channel TRPA1, a sensor for toxic lung inhalants, in pulmonary epithelial cells. Chem Biol Interact 206(3):462–471. doi:10.1016/j.cbi.2013.08.012

Centers for Disease Control and Prevention (2003) Facts about sulfur mustard (http://www.cdc.gov/niosh/ershdb/EmergencyResponseCard_29750008.html)

de la Roche J, Eberhardt MJ, Klinger AB, Stanslowksy N, Wegner F, Koppert W, Reeh PW, Lampert A, Fischer MJM, Leffler A (2013) The molecular basis for species-specific activation of human TRPA1 by protons involves poorly conserved residues within transmembrane domains 5 and 6. J Biol Chem. doi:10.1074/jbc.M113.479337

Defalco J, Steiger D, Gustafson A, Emerling DE, Kelly MG, Duncton MAJ (2010) Oxime derivatives related to AP18: agonists and antagonists of the TRPA1 receptor. Bioorg Med Chem Lett 20(1):276–279. doi:10.1016/j.bmcl.2009.10.113

Dons D (2013) As Syria crisis mounts, scientist looks back at last major chemical attack. Science 341(6150):1051. doi:10.1126/science.341.6150.1051

Fernandes ES, Fernandes MA, Keeble JE (2012) The functions of TRPA1 and TRPV1: moving away from sensory nerves. Br J Pharmacol 166(2):510–521. doi:10.1111/j.1476-5381.2012.01851.x

Finkelman FD (2014) Diesel exhaust particle exposure during pregnancy promotes development of asthma and atopy. J Allergy Clin Immunol. doi:10.1016/j.jaci.2014.04.002

Gautam A, Vijayaraghavan R, Sharma M, Ganesan K (2006) Comparative toxicity studies of sulfur mustard (2,2′-dichloro diethyl sulfide) and monofunctional sulfur mustard (2-chloroethyl ethyl sulfide), administered through various routes in mice. J Med CBR Def 4. http://www.jmedcbr.org/issue_0401/Vijay/Vijay_02_06.html

Gazdar AF, Oie HK, Shackleton CH, Chen TR, Triche TJ, Myers CE, Chrousos GP, Brennan MF, Stein CA, La Rocca RV (1990) Establishment and characterization of a human adrenocortical carcinoma cell line that expresses multiple pathways of steroid biosynthesis. Cancer Res 50:5488–5496

Ghanei M, Rajaeinejad M, Motiei-Langroudi R, Alaeddini F, Aslani J (2011) Helium:oxygen versus air:oxygen noninvasive positive-pressure ventilation in patients exposed to sulfur mustard. Heart Lung 40(3):e84–e89. doi:10.1016/j.hrtlng.2010.04.001

Hinman A, Chuang H, Bautista DM, Julius D (2006) TRP channel activation by reversible covalent modification. Proc Natl Acad Sci USA 103(51):19564–19568. doi:10.1073/pnas.0609598103

Hoenig SL (2002) Handbook of chemical warfare and terrorism. Greenwood Press, Connecticut

Jordt S, Bautista DM, Chuang H, McKemy DD, Zygmunt PM, Hogestatt ED, Meng ID, Julius D (2004) Mustard oils and cannabinoids excite sensory nerve fibres through the TRP channel ANKTM1. Nature 427(6971):260–265. doi:10.1038/nature02282

Kehe K, Balszuweit F, Steinritz D, Thiermann H (2009) Molecular toxicology of sulfur mustard-induced cutaneous inflammation and blistering. Toxicology 263(1):12–19. doi:10.1016/j.tox.2009.01.019

Kendall JM, Badminton MN (1998) *Aequorea victoria* bioluminescence moves into an exciting new era. Trends Biotechnol 16(5):216–224. doi:10.1016/S0167-7799(98)01184-6

Kinnamon SC (2012) Taste receptor signalling—from tongues to lungs. Acta Physiol (Oxf) 204(2):158–168. doi:10.1111/j.1748-1716.2011.02308.x

Macpherson LJ, Dubin AE, Evans MJ, Marr F, Schultz PG, Cravatt BF, Patapoutian A (2007) Noxious compounds activate TRPA1 ion channels through covalent modification of cysteines. Nature 445(7127):541–545. doi:10.1038/nature05544

McManus J, Huebner K (2005) Vesicants. Crit Care Clin 21(4):707–718 vi. doi: 10.1016/j.ccc.2005.06.005

Mukhopadhyay I, Gomes P, Aranake S, Shetty M, Karnik P, Damle M, Kuruganti S, Thorat S, Khairatkar-Joshi N (2011) Expression of functional TRPA1 receptor on human lung fibroblast and epithelial cells. J Recept Signal Transduct Res 31(5):350–358. doi:10.3109/10799893.2011.602413

Nakatsuka K, Gupta R, Saito S, Banzawa N, Takahashi K, Tominaga M, Ohta T (2013) Identification of molecular determinants for a potent mammalian TRPA1 antagonist by utilizing species differences. J Mol Neurosci 51(3):754–762. doi:10.1007/s12031-013-0060-2

Nassini R, Pedretti P, Moretto N, Fusi C, Carnini C, Facchinetti F, Viscomi AR, Pisano AR, Stokesberry S, Brunmark C, Svitacheva N, McGarvey L, Patacchini R, Damholt AB, Geppetti P, Materazzi S, Guerrero-Hernandez A (2012) Transient receptor potential ankyrin 1 channel localized to non-neuronal airway cells promotes non-neurogenic inflammation. PLoS One 7(8):e42454. doi:10.1371/journal.pone.0042454

Nilius B, Appendino G, Owsianik G (2012) The transient receptor potential channel TRPA1: from gene to pathophysiology. Pflug Arch 464(5):425–458. doi:10.1007/s00424-012-1158-z

Noort D, Fidder A, Degenhardt-Langelaan CEAM, Hulst AG (2008) Retrospective detection of sulfur mustard exposure by mass spectrometric analysis of adducts to albumin and hemoglobin: an in vivo study. J Anal Toxicol 32(1):25–30. doi:10.1093/jat/32.1.25

Pechura CM, Rall DP (1993) Veterans at risk: the health effects of mustard gas and lewisite. National Academy Press, Washington, DC

Petrus M, Peier AM, Bandell M, Hwang SW, Huynh T, Olney N, Jegla T, Patapoutian A (2007) A role of TRPA1 in mechanical hyperalgesia is revealed by pharmacological inhibition. Mol Pain 3:40. doi:10.1186/1744-8069-3-40

Pohanka M (2012) Antioxidants countermeasures against sulfur mustard. MRMC 12(8):742–748. doi:10.2174/138955712801264783

Ramsey IS, Delling M, Clapham DE (2006) An introduction to TRP channels. Annu Rev Physiol 68:619–647. doi:10.1146/annurev.physiol.68.040204.100431

Riccardi M (2003) Toxicological profile for sulfur mustard (UPDATE). U.S. Department of Health and Human Services 2003

Rürup R, Schieder W, Kaufmann D (2000) Geschichte der Kaiser-Wilhelm-Gesellschaft im Nationalsozialismus. Wallstein, Göttingen

Sawyer TW, Hamilton MG (2000) Effect of intracellular calcium modulation on sulfur mustard cytotoxicity in cultured human neonatal keratinocytes. Toxicol In Vitro 14(2):149–157

Schaefer EA, Stohr S, Meister M, Aigner A, Gudermann T, Buech TR (2013) Stimulation of the chemosensory TRPA1 cation channel by volatile toxic substances promotes cell survival of small cell lung cancer cells. Biochem Pharmacol 85(3):426–438. doi:10.1016/j.bcp.2012.11.019

Schmaltz F (2005) Kampfstoff-Forschung im Nationalsozialismus: Zur Kooperation von Kaiser-Wilhelm-Instituten, Militär und Industrie. Geschichte der Kaiser-Wilhelm-Gesellschaft im Nationalsozialismus, Bd. 11. Wallstein, Göttingen

Shigetomi E, Jackson-Weaver O, Huckstepp RT, O'Dell TJ, Khakh BS (2013) TRPA1 channels are regulators of astrocyte basal calcium levels and long-term potentiation via constitutive D-serine release. J Neurosci 33(24):10143–10153. doi:10.1523/JNEUROSCI.5779-12.2013

Shimomura O, Johnson FH, Morise H (1974) Mechanism of the luminescent intramolecular reaction of aequorin. Biochemistry 13(16):3278–3286. doi:10.1021/bi00713a016

Sidell FR, Urbanetti JS, Smith WJ, Hurst CG (eds) (1997) Medical aspects of chemical and biological warfare: chapter 7: vesicants. Office of the Surgeon General, Borden Institute, Walter Reed Army Medical Center Washington, DC. Office of The Surgeon General United States Army

Simon SA, Liedtke W (2008) How irritating: the role of TRPA1 in sensing cigarette smoke and aerogenic oxidants in the airways. J Clin Investig. doi:10.1172/JCI36111

Stewart CE (2006) Weapons of mass casualties and terrorism response handbook. Jones and Bartlett, Sudbury, MA

Tewari-Singh N, Inturi S, Jain AK, Agarwal C, Orlicky DJ, White CW, Agarwal R, Day BJ (2014) Catalytic antioxidant AEOL 10150 treatment ameliorates sulfur mustard analog 2-chloroethyl ethyl sulfide-associated cutaneous toxic effects. Free Radic Biol Med 72:285–295. doi:10.1016/j.freeradbiomed.2014.04.022

Thiermann H, Worek F, Kehe K (2013) Limitations and challenges in treatment of acute chemical warfare agent poisoning. Chem Biol Interact 206(3):435–443. doi:10.1016/j.cbi.2013.09.015

Veress LA, O'Neill HC, Hendry-Hofer TB, Loader JE, Rancourt RC, White CW (2010) Airway obstruction due to bronchial vascular injury after sulfur mustard analog inhalation. Am J Respir Crit Care Med 182(11):1352–1361. doi:10.1164/rccm.200910-1618OC

Wang YY, Chang RB, Allgood SD, Silver WL, Liman ER (2011) A TRPA1-dependent mechanism for the pungent sensation of weak acids. J Gen Physiol 137(6):493–505. doi:10.1085/jgp.201110615

Wilson SR, Gerhold KA, Bifolck-Fisher A, Liu Q, Patel KN, Dong X, Bautista DM (2011) TRPA1 is required for histamine-independent, Mas-related G protein-coupled receptor-mediated itch. Nat Neurosci 14(5):595–602. doi:10.1038/nn.2789

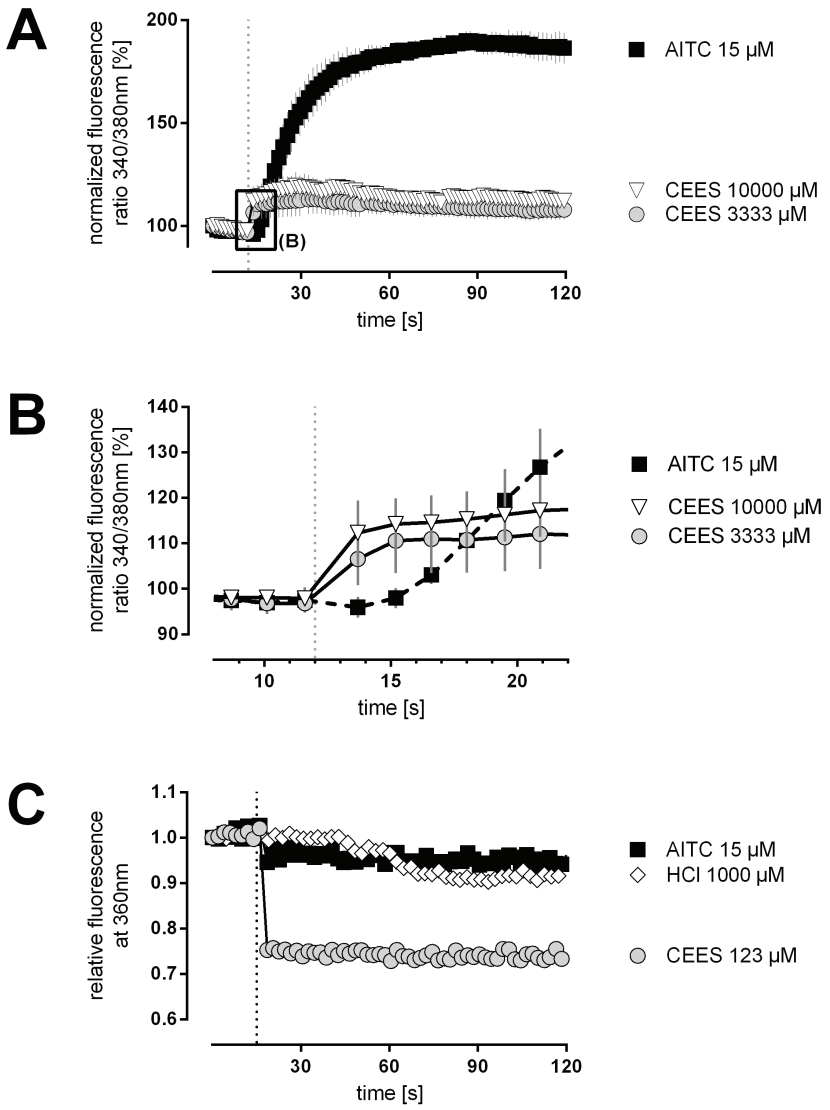

Suppl. Figure 1: HEK293-A1-E cells were loaded with Fura-2 AM and stimulated with AITC or exposed to CEES. (A) As expected, 15 µM AITC stimulation (black squares) resulted in a distinct increase of 340/380 nm fluorescence ratio, indicating a pronounced calcium influx. Exposure of HEK293-A1-E cells to 10,000 µM (white triangles) or 3,333 µM CEES (gray circles) initially increased the 340/380 nm fluorescence ratio without concentration–response relationships or changes over time. (B) Zoom of (A): Moreover, the CEES-induced increase in Fura-2 AM fluorescence occurred even faster than in AITC-positive controls, suggesting chemical interference of CEES and Fura-2 AM. (C) 15 µM AITC stimulation had no influence on fluorescence emission at the isosbestic wavelength (360 nm), whereas even low concentrations of CEES (1,111-µm white triangles and 123-µM gray circles) showed a concentration-dependent decrease in fluorescence. This indicates a chemical interference of CEES with Fura-2 AM. HCl (1,000 µM, white diamonds) did not affect Fura-2 AM fluorescence at 360 nm, underlining our hypothesis of a CEES-induced Fura-2 AM modification.

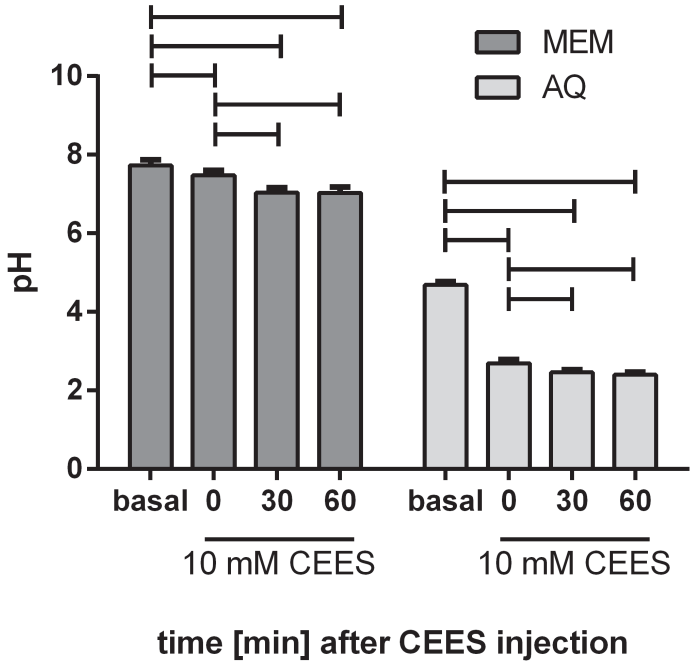

Suppl. Figure 2: Acidification, i.e., decrease in pH values, following the hydrolysis of 10,000 µM CEES in MEM or distilled water (AQ). In AQ, almost immediate hydrolysis occurs, lowering the pH from 4.7 to 2.7. This corresponds to a 100x increase in proton concentration. After 30 min, the pH value decreased to 2.4 and remained almost unchanged afterward. In MEM, pH values decreased only slightly from 7.7 to 7.5 immediately after adding 10,000 µM CEES and to 7.0 after 30 or 60 min. The low concentration of free protons, present in MEM, was not even doubled, due to the buffer capacity of supplemented MEM. Horizontal bars represent significant changes ($p < 0.05$) between the groups. All experiments were conducted with n=3. Mean values ± S.D. are given.

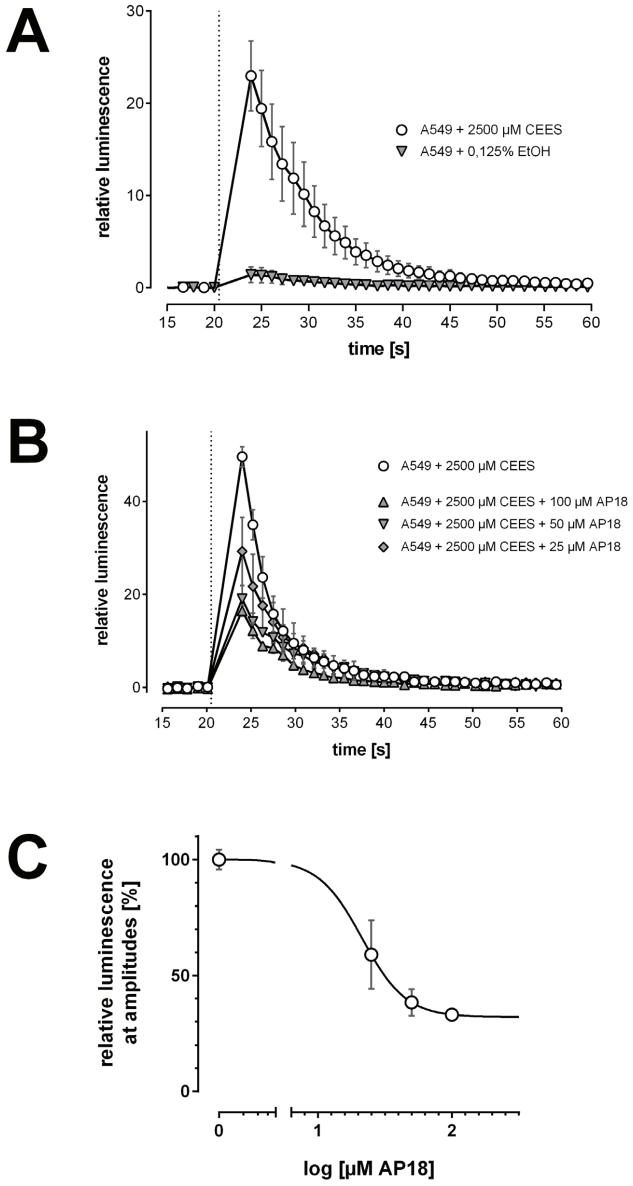

Suppl. Figure 3: (A) Human lung epithelial cells (A549) were exposed to 2,500 µM CEES (white circles) or ethanol (solvent control, gray triangles), and increase in [Ca2+]i was assessed by aequorin luminescence. A549 cells showed a distinct calcium influx after CEES exposure. Ethanol had only negligible effects. All experiments were conducted with n=3. Mean values ± S.E.M. are given. (B) Pre-incubation of A549 with AP18 at various concentrations followed by a 2,500 µM CEES exposure resulted in a significant decrease in CEES-induced calcium influx. All experiments were conducted with n=3. Mean values ± S.E.M. are given. (C) Concentration–response relationship displaying peak luminescence values (shown in Suppl. Fig. 3B) revealed a concentration-dependent effect of AP18 on CEES-induced calcium influx in A549 cells. Although a distinct decrease in calcium influx was observed, a complete inhibition could not be achieved. All experiments were conducted with n=3. Mean values ± S.E.M. are given.

3.2 *N*-Acetyl-L-Cysteine Inhibits Sulfur Mustard-Induced and TRPA1-Dependent Calcium Influx

Bernhard Stenger, Tanja Popp, Harald John, Markus Siegert, Amelie Tsoutsoulopoulos, Annette Schmidt, Harald Mückter, Thomas Gudermann, Dirk Steinritz. *Archives of Toxicology* **2016**.

The second study focused on the activation mechanism of TRPA1 channels by alkylating compounds. ROS are discussed to play a pivotal role in the cytotoxicity of SM [33, 76, 77, 78, 79]. Furthermore, TRPA1 was demonstrated to be activated by ROS [64, 80, 81, 82]. Thus, we assumed that SM-induced ROS may activate TRPA1 channels. To address that question, cells were pre-incubated with two well-established ROS scavengers, namely *N*-Acetyl-l-cysteine (NAC) and glutathione (GSH) [83, 84], prior to SM challenge. First, SM was more potent with regard to TRPA1 activation than CEES ($EC_{50\,(CEES)} = 7392\,\mu M$; $EC_{50\,(SM)} = 575\,\mu M$) (Figure 2, p. 17; Figure 1, p. 33). EC_{50} values differed from each other by a factor of 15. Remarkably, cytotoxicity in human keratinocytes exposed to CEES or SM also differed by a factor of 12 ($LC_{50\,(CEES)} = 1443\,\mu M$; $LC_{50\,(SM)} = 96\,\mu M$) [85]. Pre-incubation with NAC prevented SM-induced TRPA1 activation and followed a dose-response relationship (Figure 3, p. 34). Interestingly, GSH pretreatment did not affect SM-induced TRPA1 activation (Figure 5, p. 35). Based on these results, we excluded a significant impact of ROS on TRPA1 activation in our experiments but assumed SM-scavenging effects especially by NAC. However, FACS-analysis revealed no difference with regard to SM-DNA-adduct formation after both NAC or GSH pre-treatment (Figure 7, p. 36). To verify our results, LC-ESI MS/MS analysis of cell lysates was performed (Figure 8, p. 37; Figure 9, p. 39). Cells contained considerable levels of GSH *a priori* but no detectable NAC. Moreover, GSH or NAC levels remained unchanged despite antioxidant pretreatment. NAC-SM adducts (NAC-HETE) were not detected in lysates, however, some minor amounts of GSH-SM adducts (GSH-HETE) were identified. Nevertheless, SM scavenging did not affect DNA-SM adduct levels, as mentioned above. Obviously, NAC and GSH exhibit different properties in our experiments. Based on the mass spectrometry data that did not suggest intracellular effects of GSH or NAC, we assumed extracellular effects especially of NAC on TRPA1. Indeed, pre-incubation with NAC also prevented AITC-induced TRPA1 activation while GSH had no effect (Figure 4, p. 34; Figure 6, p. 35). Thus, we hypothesized a direct interaction between NAC and TRPA1 at reactive extracellular moieties, thereby inactivating the channel.

In summary, the key findings of this work were: (i) SM is more potent in activating TRPA1 channels compared to CEES, (ii) NAC-pre-treatment can prevent SM-induced channel activiation while GSH-pre-treatment cannot, and (iii) a direct influence of NAC on extracellular TRPA1 protein residues is assumed.

Arch Toxicol
DOI 10.1007/s00204-016-1873-x

MOLECULAR TOXICOLOGY

N-Acetyl-L-cysteine inhibits sulfur mustard-induced and TRPA1-dependent calcium influx

Bernhard Stenger[1] · Tanja Popp[1,2] · Harald John[2] · Markus Siegert[6] · Amelie Tsoutsoulopoulos[2] · Annette Schmidt[2,3] · Harald Mückter[1] · Thomas Gudermann[1,4,5] · Horst Thiermann[2] · Dirk Steinritz[1,2]

Received: 4 August 2016 / Accepted: 6 October 2016

Abstract Transient receptor potential family channels (TRPs) have been identified as relevant targets in many pharmacological as well as toxicological studies. TRP channels are ubiquitously expressed in different tissues and act among others as sensors for different external stimuli, such as mechanical stress or noxious impacts. Recent studies suggest that one member of this family, the transient receptor potential ankyrin 1 cation channel (TRPA1), is involved in pain, itch, and various diseases, suggesting TRPA1 as a potential therapeutic target. As a nociceptor, TRPA1 is mainly activated by noxious or electrophilic compounds, including alkylating substances. Previous studies already revealed an impact of 2-chloroethyl-ethyl sulfide on the ion channel TRPA1. In this study, we demonstrate that sulfur mustard (bis-(2-chloroethyl) sulfide, SM) activates the human TRPA1 (hTRPA1) in a dose-dependent manner measured by the increase in intracellular Ca^{2+} concentration ($[Ca^{2+}]_i$). Besides that, SM-induced toxicity was attenuated by antioxidants. However, very little is known about the underlying mechanisms. Here, we demonstrate that *N*-acetyl-L-cysteine (NAC) prevents SM-induced hTRPA1-activation. HEK293-A1-E cells, overexpressing hTRPA1, show a distinct increase in $[Ca^{2+}]_i$ immediately after SM exposure, whereas this increase is reduced in cells pretreated with NAC in a dose-dependent manner. Interestingly, glutathione, although being highly related to NAC, did not show an effect on hTRPA1 channel activity. Taken together, our results provide evidence that SM-dependent activation of hTRPA1 can be diminished by NAC treatment, suggesting a direct interaction of NAC and the hTRPA1 cation channel. Our previous studies already showed a correlation of hTRPA1-activation with cell damage after exposure to alkylating agents. Therefore, NAC might be a feasible approach mitigating hTRPA1-related dysregulations after exposure to SM.

Keywords TRPA1 · Sulfur mustard · NAC · GSH · Calcium signaling · HEK293

Abbreviations

AITC	Allylisothiocyanate
AP18	4-(4-Chlorophenyl)-3-methylbut-3-en-2-oxime
CEES	2-Chloroethyl-ethyl sulfide
DMEM	Dulbecco's modified Eagle medium
EDTA	Ethylenediaminetetraacetic acid
EtOH	Ethanol
FA	Formic acid
FACS	Fluorescence-activated cell sorting
FBS	Fetal bovine serum

Bernhard Stenger and Tanja Popp have contributed equally to this work.

✉ Tanja Popp
tanjajudithjulianapopp@bundeswehr.org

1 Walther-Straub-Institute of Pharmacology and Toxicology, Ludwig-Maximilians-University Munich, Goethestraße 33, 80336 Munich, Germany

2 Bundeswehr Institute of Pharmacology and Toxicology, Neuherbergstraße 11, 80937 Munich, Germany

3 Department of Molecular and Cellular Sports Medicine, German Sports University Cologne, Am Sportpark Müngersdorf 6, 50933 Cologne, Germany

4 Comprehensive Pneumology Center Munich (CPC-M), German Center for Lung Research, 81377 Munich, Germany

5 DZHK (German Centre for Cardiovascular Research), Munich Heart Alliance, 80636 Munich, Germany

6 Department of Chemistry, Humboldt-Universität zu Berlin, 12489 Berlin, Germany

Published online: 13 October 2016

GSH	Glutathione
h	Hours
HEK293-A1-E	HEK293 cells, stable transfected with hTRPA1, Clone E
HEK293-WT	HEK293 wild-type cells
HETE	Hydroxyethylthioethyl
(h)TRPA1	(human) Transient receptor potential cation channel A1
Int. (cps)	Intensity (counts per second)
iPrOH	Iso-propanol
LC-ESI MS/MS	Liquid chromatography-electrospray ionization tandem-mass spectrometry
MEM	Minimum essential medium
mM	Millimolar
µM	Micromolar
min	Minutes
MRM	Multiple reaction monitoring
NAC	*N*-Acetyl-L-cysteine
P/S	Penicillin/streptomycin
PBS	Phosphate-buffered saline
ROS	Reactive oxygen species
RT	Room temperature
s	Seconds
SEM	Standard error of the mean
SM	Sulfur mustard, bis-(2-chloroethyl) sulfide

Introduction

Sulfur mustard (SM) is a chemical warfare agent that was discovered in 1822. It was extensively used in World War I before being ostracized by the Geneva Protocol in 1925 (Hoenig 2002). Nevertheless, it was used in other military conflicts in the past, e.g., Gulf War I (Iraq–Iran 1980–1988) (Abolghasemi et al. 2010). Recent findings in Syria and current news from Iraq have documented or at least suggested that a terroristic use of SM cannot be ruled out. Thus, an imminent risk does exist (Thiermann et al. 2013; Dons 2013).

Although SM-induced skin injuries may be severe, lethality is comparably low (Maynard and Chilcott 2009). In contrast, SM-induced lung injuries may result in devastating acute health effects with fatal outcome. Blistering of lung tissue with accompanying detachment of lung epithelia can result in the formation of pseudo-membranes that may clog the airways and provoke a life-threatening situation (Kehe et al. 2009). Despite decades of medical research, neither an antidote nor a specific therapy does exist. Therapy targets primarily symptom relief (Thiermann et al. 2013). One reason for this shortcoming is the largely unknown molecular toxicology of SM and related compounds.

Recently, it was demonstrated that alkylating substances including 2-chloroethyl-ethyl sulfide (CEES), a monofunctional analog of SM, and also SM itself are able to activate transient receptor potential ankyrin 1 cation channels (TRPA1) located in the plasma membrane (Stenger et al. 2014). TRPA1 channels are part of the superfamily of transient receptor potential (TRP) ion channels and represent the only member of this subfamily (Ramsey et al. 2006). TRPA1 is ubiquitously expressed in different tissues including lung and skin, but was first found in sensory neurons (Büch et al. 2013; Atoyan et al. 2009; Story et al. 2003). Previous studies revealed that contact with pungent substances results in the activation of TRPA1 (Bandell et al. 2004). Furthermore, the cytotoxic effects of alkylating agents are related to TRPA1-activity, as a protective effect could be achieved by the inhibition of TRPA1 (Stenger et al. 2014).

Antioxidants have been reported to effectively counteract TRPA1-mediated itch and are considered beneficial in SM poisoning (Pohanka 2012; Balszuweit et al. 2015). However, the exact underlying mechanisms have not been elucidated so far. With regard to SM, direct scavenging effects as well as reactive oxygen species (ROS)-scavenging ability of *N*-acetyl-L-cysteine (NAC) or glutathione (GSH) are discussed. Whether NAC or GSH exhibit additional direct effects on TRPA1 channels has not been investigated so far. In the current study, we examined the activation of hTRPA1 channels by SM in the presence of both antioxidants NAC or GSH.

Materials and methods

Chemicals

Sulfur mustard was made available by the German ministry of Defense and tested for integrity and purity (at least 99 %) in-house by NMR. The 2F8 antibody used for FACS analysis was purchased from TNO (The Hague, The Netherlands). Dulbecco's minimal Eagle medium (DMEM), minimum essential medium (MEM), fetal bovine serum (FBS), phosphate-buffered saline (PBS), and trypsin–EDTA were purchased from Life Technologies (Gibco, Karlsruhe, Germany). *N*-Acetyl-L-cysteine (NAC), allylisothiocyanate (AITC), 2-chloroethyl-ethyl sulfide (CEES), and penicillin/streptomycin (P/S) were obtained from Sigma-Aldrich (Steinheim, Germany). PromoFectin transfection reagent was delivered from PromoCell GmbH (Heidelberg, Germany). Coelenterazine was purchased from pjk GmbH (Kleinblittersdorf, Germany). AP18 was obtained from Bio-Techne (Wiesbaden-Nordenstadt, Germany). Acetonitrile (ACN, gradient grade), iso-propanol (iPrOH, gradient grade), and water (HPLC grade) were purchased

from Merck (Darmstadt, Germany). Formic acid (FA, ≥98 % p.a. ACS) and ethanol (EtOH) were obtained from Carl Roth (Karlsruhe, Germany).

Cell lines

The generation of transfected HEK293 cells, stably expressing hTRPA1 (HEK293-A1-E), has been described previously (Schäfer et al. 2013). HEK293 wild-type (HEK293-WT) cells were kindly donated by Vladimir Chubanov (Walther-Straub-Institute, Munich, Germany). Both cell lines were cultured in DMEM, containing 4.5 g/l glucose, L-glutamine, and Earle's salts, supplemented with 10 % FBS and 1 % P/S in a humidified atmosphere at 5 % (v/v) CO_2. All cells were trypsinized for 2 min and resuspended in the respective medium every 2–3 days.

Transient transfection of Ca^{2+}-sensitive aequorin-plasmid

The aequorin-coding plasmid was kindly provided by Andreas Breit (Walther-Straub-Institute, Munich, Germany). The DNA construct (12 µg) was diluted in 500 µl minimum essential medium (MEM) without any additional supplements. PromoFectin (12 µl) was diluted in 500 µl MEM without any further supplements. Both solutions were thoroughly mixed by vortexing and incubated for 30 min at room temperature (RT). This transfection mix was then transferred into a T25 cell culture flask before 4 ml of cell suspension containing a total of 4×10^6 HEK293-A1-E cells were seeded on top. Cells were cultured for up to 4 days.

Functional measurement of Ca^{2+} influx using an aequorin-assay

Changes of $[Ca^{2+}]_i$ were measured using the calcium-sensitive photoprotein aequorin as described earlier (Shimomura et al. 1974; Kendall and Badminton 1998). In brief, a T25 flask containing aequorin-transfected cells was trypsinized and diluted in 3-ml DMEM without FBS and P/S. Afterward, HEK293-A1-E were loaded with 5 µM of the apoaequorin chromophore coelenterazine for 15 min at RT. Per well of a Greiner 96-well Lumitrac 200 Plate (Greiner Bio-One, Frickenhausen, Germany), 200 µl of the cell suspension was transferred. Chemiluminescence was recorded with an integration time of 1000 ms over 2 min using a Tecan infinite m200Pro plate reader (Tecan Group AG, Männedorf, Switzerland) equipped with a gas control module to maintain 37 °C and 5 % (v/v) CO_2 within the plate reader. Injections of 10 µl of the respective chemicals [SM, AITC (positive control), CEES or EtOH (solvent control)] were done after 15 cycles of baseline recording. To minimize hydrolysis of SM, the agent was first dissolved in EtOH at a concentration of 400 mM. Dilution in MEM just prior to the experiment resulted in the final concentrations needed in the different experiments.

Cells were incubated with the non-covalent TRP channel inhibitor AP18 for 5 min prior to SM injection. For NAC and GSH experiments, cells were pre-incubated with the antioxidants for 15 min, washed with PBS and harvested using 0.5 ml 0.25 % trypsin–EDTA. Cells were resuspended with 2.5 ml MEM resulting in a total of 3 ml cell suspension. Ca^{2+} measurements of AP18 experiments were performed in the presence of extracellular AP18.

Normalization was done by dividing raw values by the mean of the baseline resulting in a relative increase in chemiluminescence normalized to the baseline.

FACS analysis

Cells were pretreated with GSH, NAC, or PBS as a control for 20 min. Subsequently, washed cells were exposed to different concentrations of SM for 15 min. After three washing steps with PBS, cells were fixed with 0.5 % (w/v) paraformaldehyde, permeabilized and finally treated with formamide. Samples were stained with the monoclonal antibody 2F8 against N7-hydroxyethylthioethyl-2′-deoxyguanosine (N7-HETE-dG). Flow cytometry was carried out with FACS Canto II (BD Biosciences, San Jose, USA), and results were analyzed using the software FACSDiva. Specifically, stained cells but SM-untreated were used as a reference. Herein, the mean fluorescence of each sample was calculated in relation with the untreated reference.

Preparation of NAC–HETE and GSH–HETE references

NAC solution in saline (500 µl, 10 µg/ml, 61 µM) was mixed with 25 µl of SM diluted in iPrOH (12 mM) resulting in a molar ratio NAC/SM of 1:10. After reaction for 2 h at 37 °C under gentle shaking and subsequent 12 h at 4 °C, the mixture was diluted 1:10 in 0.5 % v/v FA for LC-ESI MS/MS analysis. GSH was also dissolved in 1 ml saline yielding 1 mg/ml (3 mM) and mixed with 4 µl SM resulting in a concentration of 32 mM (molar ratio GSH/SM 1:11). After 2 h reaction at 37 °C under gentle shaking, another 12 h at 4 °C followed prior to a 1:1000 dilution with 0.5 % v/v FA ready for LC-ESI MS/MS analysis in product ion scan mode (see below).

Sample preparation for LC-ESI MS/MS analysis

For analysis of NAC and GSH as well as their alkylated SM products, cell lysates were prepared according to the

following procedure. Cell suspensions were treated with 100 µM NAC or GSH for 15 min at 37 °C and 5 % (v/v) CO_2. After thorough washing with PBS, cells were exposed to 500 µM SM or the corresponding amount of EtOH as a solvent control and were allowed to incubate for 30 min at 37 °C and 5 % (v/v) CO_2. Cells were extensively washed (5×) with PBS followed by 5 × freeze/thaw cycles for cell lysis. Prior to LC-ESI MS/MS analysis, cell culture medium (blank) and lysates (100 µl each) were mixed with acetonitrile (200 µl) to precipitate any protein content. After centrifugation (5 min at 10,000 g), 200 µl of the supernatant was evaporated to dryness in glass vials under a gentle stream of nitrogen. Residues were reconstituted in 300 µl 0.5 % v/v FA. Re-dissolved lysate samples were centrifuged again to separate any particulate matter. Liquid phases were ready for LC-ESI MS/MS analysis in multiple reaction monitoring (MRM) mode.

LC-ESI MS/MS analysis

LC equipment consisted of an UltiMate 3000 Standard LC System (Dionex, Sunnyvale, CA, USA) including an UltiMate 3000 pump with an autosampler kept at 15 °C and a column compartment adjusted to 30 °C. The LC system was connected with an API 4000 QTrap mass spectrometer (AB SCIEX, Darmstadt, Germany). Using an Atlantis T3 column (150 × 2.1 mm i.d., 3 µm, 100 A, Waters, Eschborn, Germany) connected with a precolumn (security guard cartridges, widepore C18 4 × 2 mm i.d., Phenomenex, Aschaffenburg, Germany), samples (30 µl) were separated at a flow of 200 µl/min. The mobile phase consisted of solvent A (0.1 % v/v FA) and solvent B (ACN/H_2O 80:20 v/v, 0.1 % v/v FA) applied in gradient mode: t[min]/B[%]: 0/0; 3/0; 25/70; 28/70; 29/0; 30/0 with an initial 3-min equilibration period under starting conditions. MS data analysis and control of the mass spectrometer were done with the Analyst 1.6 software (AB SCIEX) and a Dionex chromatography MS link (version 2.12.0.3414).

Analysis of NAC and NAC–HETE

MS parameters were set to: curtain gas (CUR) 35 psi (2.42×10^5 Pa), ionization voltage (IS) 3500 V, temperature 500 °C, declustering potential (DP) 51 V, entrance potential (EP) 10 V, heater gas (GS1) and turbo ion spray gas (GS2) both 60 psi (4.14×10^5 Pa), and dwell time 80 ms. LC-ESI MS/MS runs in MRM mode were recorded after collision-induced dissociation (CID) with individual values of collision energy (CE) and cell exit potential (CXP) given in parenthesis below. Protonated NAC was monitored with transitions from *m/z* 164.0 to *m/z* 76.0 (CE 25 V, CXP 10 V), *m/z* 58.9 (CE 45 V, CXP 12 V), and *m/z* 43.0 (CE 45 V, CXP 12 V). NAC–HETE was detected as protonated ion with transitions from *m/z* 268.0 to *m/z* 162.0 (CE 35 V, CXP 10 V) and *m/z* 105.0 (CE 35 V, CXP 10 V). Detection of all fragments produced by CID from synthetic references was done in product ion scan mode of either *m/z* 164.0 for NAC or *m/z* 268.0 for NAC–HETE recording ions from *m/z* 50 to *m/z* 300 with a CE of 25 V.

Analysis of GSH and GSH–HETE

The following MS parameters were adjusted for GSH and GSH–HETE detection: CUR 35 psi (2.42×10^5 Pa), IS 3500 V, temperature 500 °C, EP 10 V, GS1 and GS2 both 60 psi (4.14×10^5 Pa), and dwell time 70 ms. Transitions resulting from CID of protonated GSH were measured in MRM mode from *m/z* 308.2 to *m/z* 179.0 (DP 51 V, CE 17 V, CXP 10 V), *m/z* 162.9 (DP 51 V, CE 25 V, CXP 10 V), and *m/z* 76.1 (DP 71.0 V, CE 45 V, CXP 6 V). GSH–HETE was monitored from *m/z* 412.0 to *m/z* 137.0 (DP 60 V, CE 25 V, CXP 10 V) and *m/z* 105.0 (DP 60 V, CE 25 V, CXP 10 V). Initial detection of the entire fragmentation spectrum of synthetic references was done in product ion scan mode from *m/z* 50 to *m/z* 450 with a CE of 25 V.

Statistics

Statistical analysis of all cell-associated experiments was performed using GraphPad prism version 6.02 software. For statistical comparison of the maximal response, one-way ANOVA with Bonferroni correction for multiple comparisons was chosen. *P* values <0.05 were regarded as significant.

Results

SM activates ion channel hTRPA1 in a dose-dependent manner

HEK293-A1-E cells were exposed to different concentrations of SM (12.5–5000 µM). Ca^{2+} influx was measured using a luminescence-based apoaequorin assay. SM stimulation led to an increase in the intracellular Ca^{2+} concentration ($[Ca^{2+}]_i$) following a dose–response relationship (Fig. 1a). The maximum luminescence signal was obtained at 2000 µM SM and reached a plateau without an additional increase at 3000 µM (Fig. 1a) or above (up to 5000 µM SM; data not shown). The EC_{50} was calculated at 575 µM SM (Fig. 1b) which was finally used in subsequent experiments.

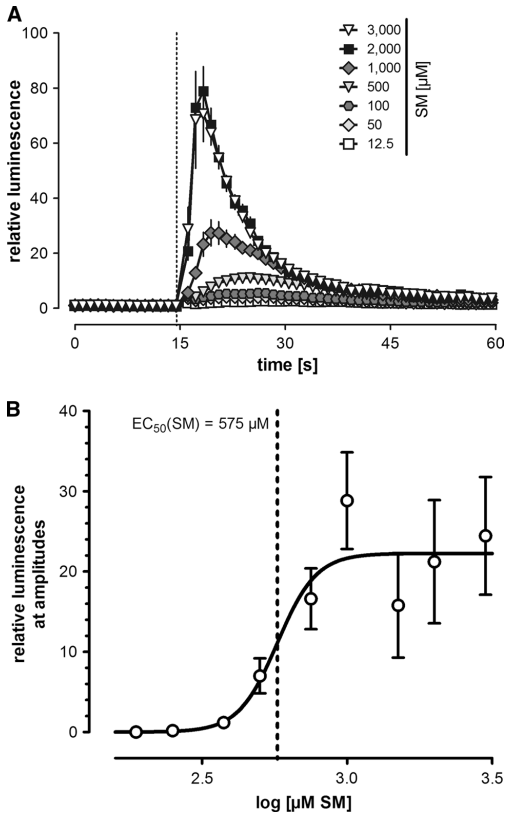

Fig. 1 **a** HEK293-A1-E cells were transfected with aequorin and loaded with 5 µM coelenterazine. Baseline luminescence was measured for 14 s subsequently. Cells were stimulated with different concentrations of SM. The *vertical dotted line* indicates the time of injection. The cells responded with an enhanced Ca^{2+} influx with increasing SM concentration. All experiments were conducted with $n = 3$. Mean values ± SEM are given. **b** Concentration–response relationship displaying peak luminescence values (shown in **a**). The EC_{50} value for SM was determined at 575 µM SM, visualized with a *dotted line*

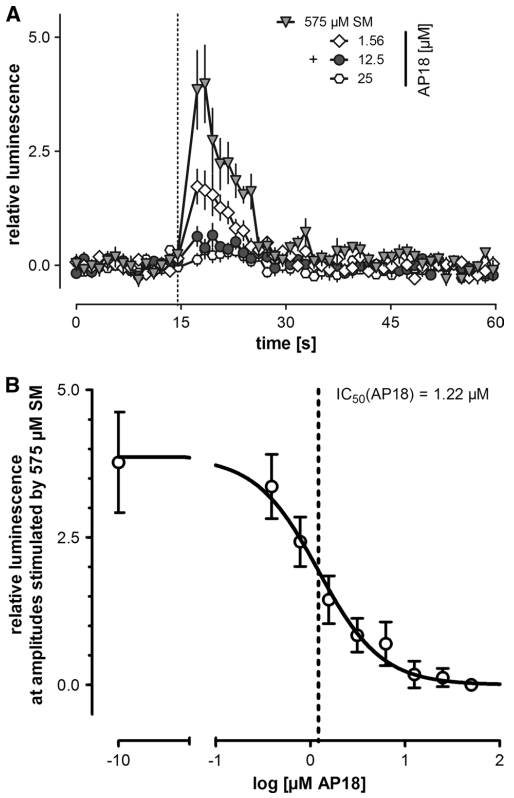

Fig. 2 **a** HEK293-A1-E cells were transfected with aequorin and loaded with 5 µM coelenterazine. Cells were then pretreated with different concentrations of the TRPA1-antagonist AP18 before being stimulated with 575 µM SM. Subsequently, luminescence was measured. The *vertical dotted line* indicates the time of injection. AP18 prevented SM-induced and TRPA1-mediated Ca^{2+} influx in a dose-dependent manner. All experiments were conducted with $n = 3$. Mean values ± SEM are given. **b** Concentration–response relationship displaying peak luminescence values (shown in **a**). The IC_{50} value was calculated at 1.22 µM AP18, visualized with a *dotted line*

AP18 blocks SM-induced increase of $[Ca^{2+}]_i$

HEK293-A1-E cells were pretreated for 5 min with different concentrations of the TRPA1-specific blocker. AP18 concentration dependently prevented SM-induced hTRPA1-activation. For complete abolishment of SM-induced TRPA1-activation, 25 µM AP18 was required (Fig. 2a). However, already, 0.78 µM AP18 could reduce SM-induced TRPA1-activation. The IC_{50} of AP18 with regard to exposure with 575 µM SM was calculated to be 1.22 µM (Fig. 2b).

NAC has antagonistic effects on TRPA1-dependent Ca^{2+} influx

HEK293-A1-E cells were pre-incubated with NAC (100, 500, or 1000 µM) for 15 min. After wash out, the cells were challenged with SM (100, 500 or 1000 µM). Pre-treatment with NAC effectively blocked the SM-induced elevation of $[Ca^{2+}]_i$ in a concentration-dependent manner (Fig. 3a, b). Strikingly, the approach with 1000 µM NAC almost completely abolished the SM-induced Ca^{2+} influx induced by all SM doses (Fig. 3a, b). Interestingly, NAC also affected

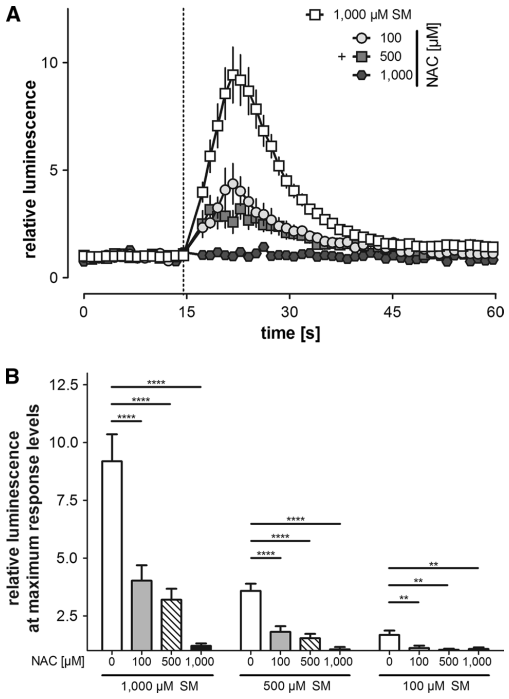

Fig. 3 **a** HEK293-A1-E cells were transfected with aequorin and loaded with 5 µM coelenterazine. Cells were pre-incubated with different NAC concentrations before challenged with 1000 µM SM. Subsequently, luminescence was measured. The *vertical dotted line marks* the time of injection. NAC was able to reduce Ca^{2+} influx in a dose-dependent manner. Ca^{2+} influx was completely inhibited by pretreating cells with 1000 µM NAC. All experiments were conducted with $n = 3$. Mean values ± SEM are given. **b** Comparison of the luminescence maxima (shown in **a**) of NAC-pretreated cells after SM exposure. Results are given as mean values ± SEM with $^{**}P < 0.01$ and $^{****}P < 0.0001$ relative to the control (set as 100 %)

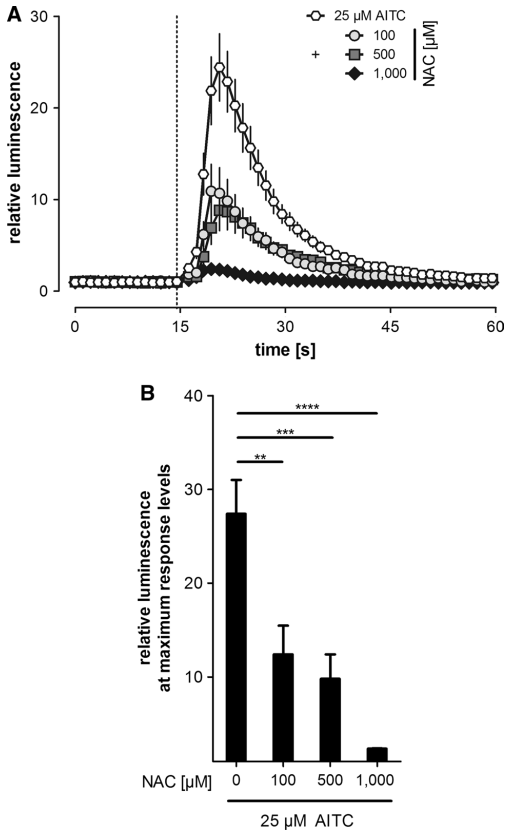

Fig. 4 **a** HEK293-A1-E cells were transfected with aequorin and loaded with 5 µM coelenterazine. The cells were incubated with increasing NAC concentrations before stimulated with 25 µM AITC. Subsequently, luminescence was measured. The *vertical dotted line marks* the time of injection. NAC was able to reduce the AITC-induced Ca^{2+} influx in a concentration-dependent manner. All experiments were conducted with $n = 3$. Mean values ± SEM are given. **b** Comparison of the luminescence maxima (shown in Fig. 8a) of NAC-pretreated cells after stimulation with 25 µM AITC. Results are given as mean values ± SEM with $^{**}P < 0.01$, $^{***}P < 0.001$ and $^{****}P < 0.0001$ relative to the control (set as 100 %)

the AITC-induced $[Ca^{2+}]_i$ response (Fig. 4a, b). The effect was again dependent on the NAC concentration comparable to SM-treated cells. Nevertheless, even with 1000 µM NAC, the Ca^{2+} influx could not be fully blocked probably due to the potency of AITC to activate TRPA1 channels. The comparison of the maximal Ca^{2+}-response levels clearly revealed a significant impact of NAC on $[Ca^{2+}]_i$ in SM- and AITC-treated cells (Figs. 3b, 4b). The same protective effect of NAC was shown for CEES-exposed cells (data not shown).

GSH has no effect on hTRPA1-dependent Ca^{2+} influx

In analogy to the NAC experiment, we investigated the influence of GSH on SM-induced hTRPA1-activation and subsequent elevation of $[Ca^{2+}]_i$. Surprisingly, preincubation with GSH followed by GSH wash out did not result in inhibition of Ca^{2+} influx in HEK293-A1-E cells after SM challenge (Fig. 5a, b). GSH had also no effect on AITC-induced hTRPA1-activation (Fig. 6a, b).

NAC and GSH do not prevent DNA-alkylation

Both NAC and GSH have been discussed as direct SM scavengers (Black et al. 1992). To test, whether this also

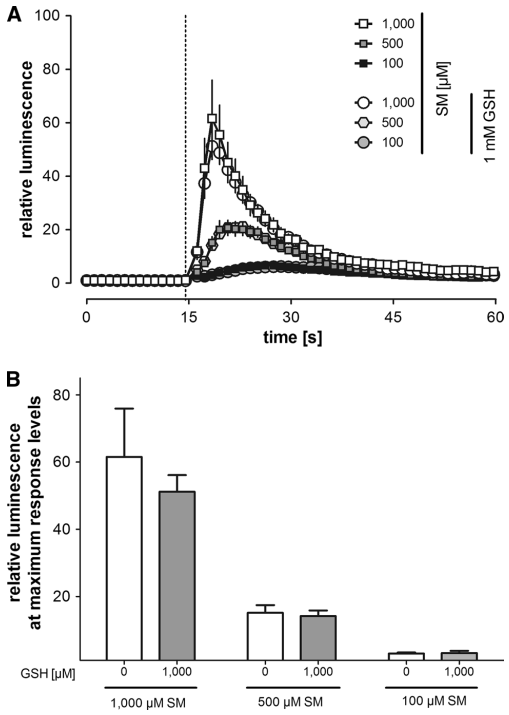

Fig. 5 **a** HEK293-A1-E cells were transfected with aequorin and loaded with 5 µM coelenterazine. Cells were pre-incubated with 1 mM GSH before exposed with different SM concentrations. Subsequently, luminescence was measured. The *vertical dotted line marks* the time of injection. GSH was not able to reduce SM-induced Ca^{2+} influx. All experiments were conducted with $n = 3$. Mean values ± SEM are given. **b** Comparison of the luminescence maxima (shown in Fig. 4a) of NAC-pretreated cells after SM exposure. No significant differences were found

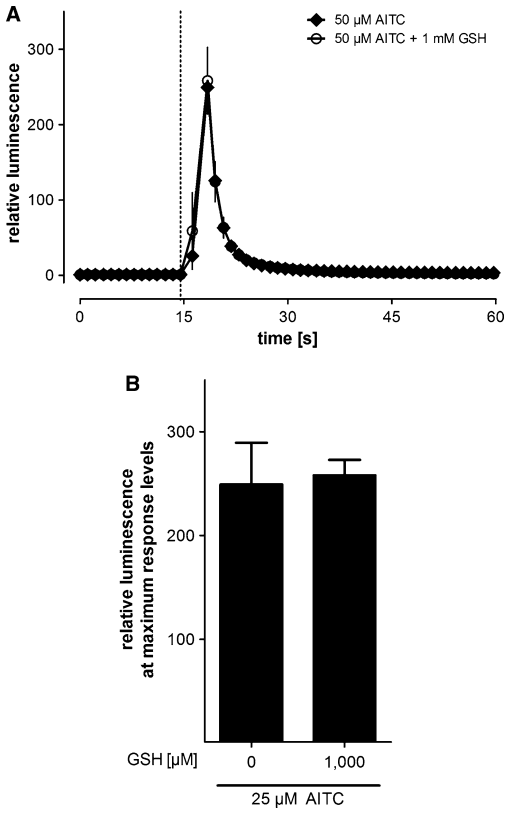

Fig. 6 **a** HEK293-A1-E cells were transfected with aequorin and loaded with 5 µM coelenterazine. The cells were incubated with 1 mM GSH before stimulated with 25 µM AITC. Subsequently, luminescence was measured. The *vertical dotted line marks* the time of injection. GSH was not able to reduce the AITC-induced Ca^{2+} influx. All experiments were conducted with $n = 3$. Mean values ± SEM are given. **b** Comparison of the luminescence maxima (shown in **a**) of GSH-pretreated cells after stimulation with 25 µM AITC. Results are given as mean values ± SEM with $^{**}P < 0.01$, $^{***}P < 0.001$ and $^{****}P < 0.0001$ relative to the control (set as 100 %)

holds true in our experiments and thus might explain the prevention of hTRPA1-activation by SM, we analyzed SM-DNA adduct formation by FACS analysis. HEK293-A1-E cells were again pre-incubated with either NAC or GSH for 15 min prior to a 15 min SM exposure. SM-DNA adducts were visualized by antibody staining and FACS analysis. The presence of NAC or GSH had no effect on SM-adduct formation (Fig. 7a, b). These data strongly suggest that both antioxidants do not act as SM scavengers within the cells in our experiments.

LC-ESI MS/MS analysis of intracellular GSH- and NAC–SM adducts

To further elucidate the scavenging potential of NAC or GSH, LC-ESI MS/MS analysis was performed. Both, NAC and GSH contain cysteine residues that might react with SM, thus preventing other reactions of SM. HEK293-A1-E cells were pre-incubated with 100 µM NAC or GSH prior to 500 µM SM challenge. As expected, cells exhibited distinct levels of GSH under basal conditions (Fig. 8b). In contrast, NAC was not detectable in these cells (Fig. 9b). Cell lysates did not reveal an increase in the amount of both antioxidants inside the pretreated cells, suggesting no excessive uptake (Figs. 8c, 9c). After SM challenge, some SM-GSH adducts (GSH–HETE) were detectable in cell lysates (Fig. 8e), whereas no SM-NAC adducts (NAC–HETE) were present (Fig. 9e). Although cells were

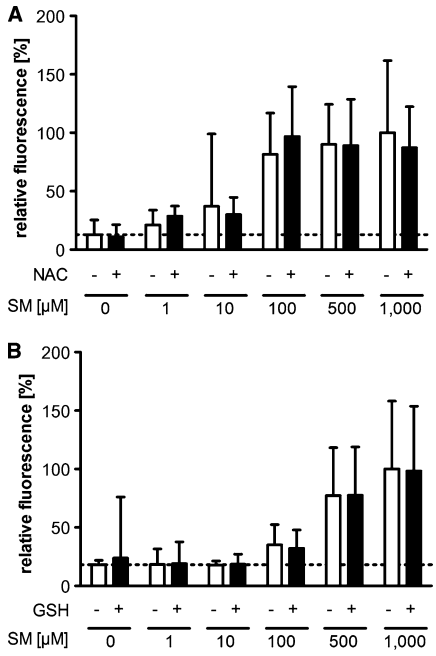

Fig. 7 **a** Cells were pre-incubated with given concentrations NAC for 15 min before exposed to different SM concentrations. Subsequently, cells were stained with 2F8 antibody against N7-HETE-dG and analyzed by flow cytometry. Relative fluorescence units are shown on the *Y*-axis. The *dotted line* indicates basal values. No difference between NAC-pre-treatment and control. Only SM challenge was detected, indicating no change in SM nucleotoxicity. **b** The cells were stained as described in **a**, only pre-incubation was performed using GSH instead of NAC. Again no difference between GSH-pre-treatment and control, but SM challenge could be observed

repeatedly washed after antioxidant pre-treatment, both GSH–HETE and to some minor extent NAC–HETE were measured in the wash fraction (Figs. 8f, 9f).

Discussion

Previous studies have demonstrated that the monofunctional alkylating agent CEES, a model substance for SM, was capable of activating hTRPA1. Moreover, hTRPA1-overexpression was associated with increased sensitivity toward CEES. Cytotoxicity was significantly attenuated by the use of specific TRPA1-blockers (Stenger et al. 2014). In this study, we investigated effects of the bifunctional alkylating agent SM on hTRPA1 channels. In line with our previous results, SM also activated hTRPA1 channels. SM turned out to be more potent compared to CEES which is reflected by an EC_{50} of 575 µM for SM compared to 7400 µM for CEES. An elevation of $[Ca^{2+}]_i$ in HEK293-A1-E cells was already observed after exposure to 50 µM SM, whereas a 10-fold higher CEES concentration (500 µM CEES) was needed for a comparable effect. Similar findings were found for the maximal Ca^{2+} influx. A plateau was reached at around 1000 µM SM, whereas CEES concentrations between 10,000 and 30,000 µM CEES were required. Although we did not investigate SM toxicity in the presented study, we demonstrated in own studies that SM is about 10-fold more toxic than CEES which correlates with the TRPA1 channel activation potential (Shakarjian et al. 2010; Sayer et al. 2010; Mangerich et al. 2016).

As reported previously, inhibition of hTRPA1 by the highly specific blocker AP18 diminished CEES-induced elevation of $[Ca^{2+}]_i$ (Stenger et al. 2014). The IC_{50} was calculated to be 0.6 µM AP18 for CEES and 1.2 µM AP18 for SM when both agents were used at their respective EC_{50} concentrations of 7400 µM CEES and 575 µM SM. These results indicate that AP18 represents a potent TRPA1-inhibitor for both CEES and SM.

The exact mechanism of TRPA1-activation by alkylating agents is still unclear. Covalent modifications of free cysteine residues, ROS-dependent mechanisms, or other interactions are conceivable. It is generally accepted, although not fully investigated, that SM exposure results in enhanced ROS production. ROS are known to activate TRPA1; therefore, they have to be considered as possible activators in the experiment (Naghii 2002; Sullivan et al. 2015). Antioxidants like NAC or GSH are well established ROS scavengers (Sies 1997; Vertuani et al. 2004). Therefore, some authors suggested the use of thiol compounds such as NAC as an antidote for treatment of SM poisoning (Bobb et al. 2005; Laskin et al. 2010; Balszuweit et al. 2015). We investigated in our experiments whether the antioxidants NAC or GSH had any effects on SM-induced Ca^{2+} influx. Cells pretreated with 1000 µM NAC did not respond with a Ca^{2+} influx even after a 1000 µM SM challenge. Prior to SM administration, NAC had been washed out to prevent sequestration of SM in supernatants. However, some very little amount of SM-NAC adducts were still found in the last washing fraction. NAC, attached to the outer cell membrane or associated with TRPA1, might be responsible for that finding. Nevertheless, based on our MS data, a significant scavenger effect of NAC is highly unlikely. Lower NAC concentrations (500 or 100 µM) were also found to be very effective in significantly attenuating the elevation of the $[Ca^{2+}]_i$. Remarkably, 100 µM NAC completely diminished the effect of 100 µM SM, representing a severe challenge, in this context.

Surprisingly, GSH at any concentration used had no effect on SM-induced and hTRPA1-mediated changes of $[Ca^{2+}]_i$. Although other studies have shown that GSH efficiently protects keratinocytes from CEES-toxicity which

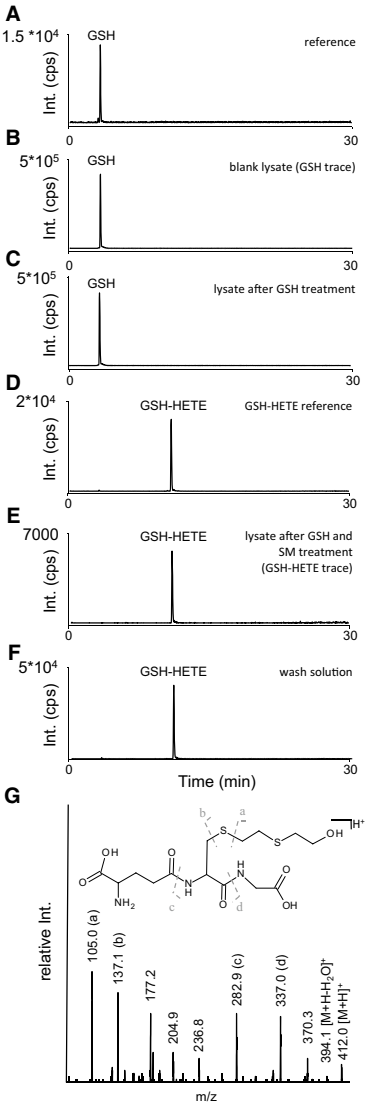

Fig. 8 GSH and GSH–HETE were detected in multiple reaction ▶ mode monitoring transitions from *m/z* 308.2 to *m/z* 179.0, *m/z* 162.9, and *m/z* 76.1 for GSH and from *m/z* 412.0 to *m/z* 137.0 and *m/z* 105.0 for NAC–HETE. For reasons of clarity, only one trace each is shown (GSH > *m/z* 179.0; GSH–HETE > *m/z* 137.0). Separations were carried out by gradient reversed-phase chromatography using an Atlantis T3 column (150 × 1.0 mm i.d., 3 µm, 100 A) at 30 °C (200 µ6/min) resulting in retention times of 3.2 min for GSH and 10.9 min for GSH–HETE. **a** GSH reference dissolved in 0.5 % v/v FA (1 µM, 307 ng/ml). **b** Blank cell lysate from cells not treated with GSH. **c** Cell lysate from cells treated with 100 µM GSH. **d** GSH–HETE reference obtained from direct reaction of GSH and SM. **e** Cell lysate from cells treated with 100 µM GSH and 500 µM SM. **f** Last wash solution of cells treated with 100 µM GSH and 500 µM SM. **g** MS/MS spectrum of GSH–HETE extracted from a LC-ESI MS/MS run in product ion scan mode of *m/z* 412.0. Sites of fragmentation (**a**–**d**) are marked and assigned to signals

was attributed to ROS-scavenging properties of GSH (Paromov et al. 2008, 2011), we presume that ROS are not the main mediators of hTRPA1-activation after SM challenge.

Moreover, our results demonstrated that pre-treatment of our cells seems not to enhance intracellular NAC- or GSH-levels beyond endogenous levels. For the very first time, the spectra of HETE-adducts of both antioxidants were analyzed by mass spectrometry revealing at least a minor scavenging function of GSH in the cell. However, since the content of SM-DNA adducts remains unchanged despite NAC- or GSH-treatment, we can exclude a direct intracellular scavenging reaction between SM and the antioxidants. Thus, the observed effects in our experiments cannot be explained by a decreased bioavailability of SM.

The covalent modification of cysteine and lysine residues within the cytosolic N-terminal domain of hTRPA1 has been identified to result in channel activation (Paulsen et al. 2015). Moreover, disulfide-bridges formed by these cysteine residues are important for the stabilization of the TRPA1 conformational state and the accessibility of TRPA1 for known activators in vivo (Wang et al. 2012). Since GSH and NAC carry a reducing thiol group, it can be speculated that both may interact with cysteine or lysine moieties, e.g., by disrupting N-terminal disulfide, thus modulating TRPA1 structure and function. However, in our LC-ESI MS/MS experiment, we were unable to detect a significant increase in intracellular concentration of NAC or GSH after pre-treatment. It may be conceivable that minute amounts, which would be below the lower limit of detection in mass spectrometry analysis, are sufficient to interfere with intracellular cysteine or lysine residues. However, this assumption is not very compelling.

Nevertheless, we observed a striking reduction in Ca^{2+} influx in cells pretreated with NAC also after stimulation with AITC. Since AITC is well described in the literature as an agonist with high specificity for the hTRPA1, we suppose an additional, more direct mechanism of NAC with regard to hTRPA1 ion channel function (Jordt et al. 2004). In accordance with this hypothesis, others previously showed that NAC can lower the affinity of the TNF receptor to its ligand TNFα independently of its antioxidant function (Hayakawa et al. 2003). Consequently, NAC might also interact with the hTRPA1 channel at extracellular or intra-membrane sites, thus, e.g., blocking the pore region or changing channel conformation. The resolved structure of TRPA1 revealed a short S1-S2 linker with solvent-accessible sites that extend into the extracellular space displaying a possible binding site (Paulsen et al. 2015). Beyond

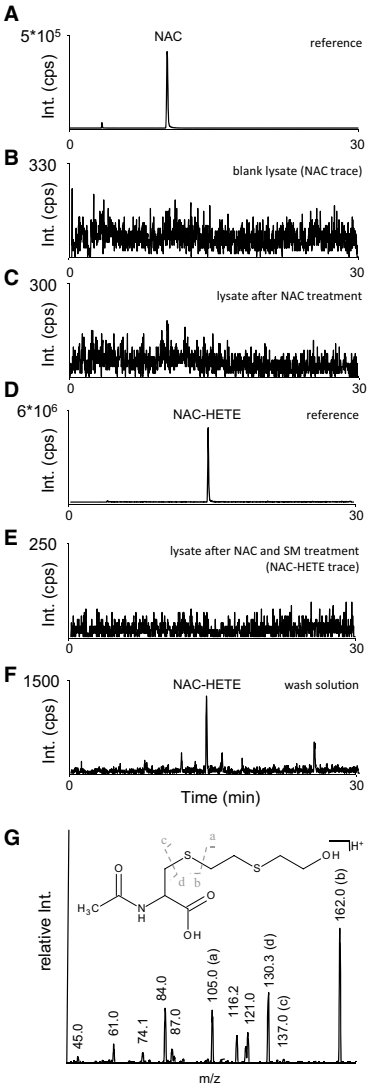

◀ **Fig. 9** NAC and NAC–HETE were detected in multiple reaction mode monitoring transitions from *m/z* 164.0 to *m/z* 76.0, *m/z* 58.9, and *m/z* 43.0 for NAC and from *m/z* 268.0 to *m/z* 162.0 and *m/z* 105.0 for NAC–HETE. For reasons of clarity, only one trace each is shown (NAC > *m/z* 76.0; NAC–HETE > *m/z* 162.0). Separations were carried out by gradient reversed-phase chromatography using an Atlantis T3 column (150 × 1.0 mm i.d., 3 µm, 100 A) at 30 °C (200 µl/min) resulting in retention times of 10.3 min for NAC and 14.2 min for NAC–HETE. **a** NAC reference dissolved in 0.5 % v/v FA (1 µM, 163 ng/ml). **b** Blank cell lysate from cells not treated with NAC. **c** Cell lysate from cells treated with 100 µM NAC. **d** NAC–HETE reference obtained from direct reaction of NAC and SM. **e** Cell lysate from cells treated with 100 µM NAC and 500 µM SM. **f** Last wash solution of cells treated with 100 µM NAC and 500 µM SM. **g** MS/MS spectrum of NAC–HETE extracted from a LC-ESI MS/MS run in product ion scan mode of *m/z* 268.0. Sites of fragmentation (**a**–**d**) are marked and assigned to signals

that, a connection of this extracellular part to the intracellular ankyrin binding motifs (well-described binding sites for AITC and other agonists) was discovered which could allow a crosstalk between extra- and intracellular parts of the channel (Paulsen et al. 2015; Hinman et al. 2006) thereby influencing the reactivity of the channel. This complex question cannot be answered at this point but will be addressed in future studies.

In conclusion, using the hTRPA1-overexpressing cell line HEK293-A1-E, we have demonstrated in the present study that SM triggers the Ca^{2+} influx specifically through hTRPA1 ion channels. Ca^{2+} signals were effectively inhibited by pre-treatment with NAC. GSH, albeit derived from NAC, does not mimic this effect pointing to distinct differences between the antioxidants. Although the exact mode of action of NAC on hTRPA1 has to be evaluated in future studies, our findings emphasize that NAC may have additional effects beyond its well-characterized role in oxidative stress scenarios. Overall, our results indicate new therapeutic approaches to protect cells against SM.

Acknowledgments We thank Ram Prasad for his excellent technical support.

Funding This research was supported by a contract (E/UR2 W/CF504/CF560) of the German Armed Forces and by Collaborative Research Center TRR 152.

Compliance with ethical standards

Conflict of interest The authors declare no conflict of interest.

References

Abolghasemi H, Radfar MH, Rambod M, Salehi P, Ghofrani H, Soroush MR, Falahaty F, Tavakolifar Y, Sadaghianifar A, Khademolhosseini SM, Kavehmanesh Z, Joffres M, Burkle FM Jr, Mills EJ (2010) Childhood physical abnormalities following paternal exposure to sulfur mustard gas in Iran: a case–control study. Confl Health 4:13. doi:10.1186/1752-1505-4-13

Atoyan R, Shander D, Botchkareva NV (2009) Non-neuronal expression of transient receptor potential type A1 (TRPA1) in human skin. J Invest Dermatol 129(9):2312–2315. doi:10.1038/jid.2009.58

Balszuweit F, Menacher G, Schmidt A, Kehe K, Popp T, Worek F, Thiermann H, Steinritz D (2015) Protective effects of the thiol compounds GSH and NAC against sulfur mustard toxicity in a human keratinocyte cell line. Toxicol Lett 244:35–43. doi:10.1016/j.toxlet.2015.09.002

Bandell M, Story GM, Hwang SW, Viswanath V, Eid SR, Petrus MJ, Earley TJ, Patapoutian A (2004) Noxious cold ion channel

TRPA1 is activated by pungent compounds and bradykinin. Neuron 41(6):849–857. doi:10.1016/S0896-6273(04)00150-3

Black RM, Brewster K, Clarke RJ, Harrison JM (1992) The chemistry of 1,1′-thiobis (2-chloroethane) (sulphur mustard) part II. 1 The synthesis of some conjugates with cysteine, *N*-acetylcysteine and *N*-acetylcysteine methyl ester. Phosphorus Sulfur Silicon Relat Elem 71(1–4):49–58. doi:10.1080/10426509208034495

Bobb AJ, Arfsten DP, Jederberg WW (2005) *N*-Acetyl-L-cysteine as prophylaxis against sulfur mustard. Mil Med 170(1):52–56. doi:10.7205/MILMED.170.1.52

Büch TRH, Schäfer EAM, Demmel M, Boekhoff I, Thiermann H, Gudermann T, Steinritz D, Schmidt A (2013) Functional expression of the transient receptor potential channel TRPA1, a sensor for toxic lung inhalants, in pulmonary epithelial cells. Chem Biol Interact 206(3):462–471. doi:10.1016/j.cbi.2013.08.012

Dons D (2013) As Syria crisis mounts, scientist looks back at last major chemical attack. Science 341(6150):1051. doi:10.1126/science.341.6150.1051

Hayakawa M, Miyashita H, Sakamoto I, Kitagawa M, Tanaka H, Yasuda H, Karin M, Kikugawa K (2003) Evidence that reactive oxygen species do not mediate NF-kappaB activation. EMBO J 22(13):3356–3366. doi:10.1093/emboj/cdg332

Hinman A, Chuang H, Bautista DM, Julius D (2006) TRP channel activation by reversible covalent modification. Proc Natl Acad Sci USA 103(51):19564–19568. doi:10.1073/pnas.0609598103

Hoenig SL (2002) Handbook of Chemical Warfare and Terrorism. Greenwood Press, Connecticut

Jordt S, Bautista DM, Chuang H, McKemy DD, Zygmunt PM, Hogestatt ED, Meng ID, Julius D (2004) Mustard oils and cannabinoids excite sensory nerve fibres through the TRP channel ANKTM1. Nature 427(6971):260–265. doi:10.1038/nature02282

Kehe K, Balszuweit F, Steinritz D, Thiermann H (2009) Molecular toxicology of sulfur mustard-induced cutaneous inflammation and blistering. Toxicology 263(1):12–19. doi:10.1016/j.tox.2009.01.019

Kendall JM, Badminton MN (1998) Aequorea victoria bioluminescence moves into an exciting new era. Trends Biotechnol 16(5):216–224. doi:10.1016/S0167-7799(98)01184-6

Laskin JD, Black AT, Jan Y, Sinko PJ, Heindel ND, Sunil V, Heck DE, Laskin DL (2010) Oxidants and antioxidants in sulfur mustard-induced injury. Ann NY Acad Sci 1203:92–100. doi:10.1111/j.1749-6632.2010.05605.x

Mangerich A, Debiak M, Birtel M, Ponath V, Balszuweit F, Lex K, Martello R, Burckhardt-Boer W, Strobelt R, Siegert M, Thiermann H, Steinritz D, Schmidt A, Burkle A (2016) Sulfur and nitrogen mustards induce characteristic poly(ADP-ribosyl)ation responses in HaCaT keratinocytes with distinctive cellular consequences. Toxicol Lett 244:56–71. doi:10.1016/j.toxlet.2015.09.010

Maynard RL, Chilcott RP (2009) Toxicology of chemical warfare agents. In: Ballantyne B, Marrs TC, Syversen T (eds) General and applied toxicology. Wiley, Chichester

Naghii MR (2002) Sulfur mustard intoxication, oxidative stress, and antioxidants. Mil Med 167(7):573–575

Paromov V, Qui M, Yang H, Smith M, Stone WL (2008) The influence of *N*-acetyl-L-cysteine on oxidative stress and nitric oxide synthesis in stimulated macrophages treated with a mustard gas analogue. BMC Cell Biol 9(1):33. doi:10.1186/1471-2121-9-33

Paromov V, Kumari S, Brannon M, Kanaparthy NS, Yang H, Smith MG, Stone WL (2011) Protective effect of liposome-encapsulated glutathione in a human epidermal model exposed to a mustard gas analog. J Toxicol 2011:109516. doi:10.1155/2011/109516

Paulsen CE, Armache J, Gao Y, Cheng Y, Julius D (2015) Structure of the TRPA1 ion channel suggests regulatory mechanisms. Nature 525(7570):552. doi:10.1038/nature14871

Pohanka M (2012) Antioxidants countermeasures against sulfur mustard. MRMC 12(8):742–748. doi:10.2174/138955712801264783

Ramsey IS, Delling M, Clapham DE (2006) An introduction to TRP channels. Annu Rev Physiol 68:619–647. doi:10.1146/annurev.physiol.68.040204.100431

Sayer NM, Whiting R, Green AC, Anderson K, Jenner J, Lindsay CD (2010) Direct binding of sulfur mustard and chloroethyl ethyl sulphide to human cell membrane-associated proteins; implications for sulfur mustard pathology. J Chromatogr B Anal Technol Biomed Life Sci 878(17–18):1426–1432. doi:10.1016/j.jchromb.2009.11.030

Schäfer EAM, Stohr S, Meister M, Aigner A, Gudermann T, Buech TRH (2013) Stimulation of the chemosensory TRPA1 cation channel by volatile toxic substances promotes cell survival of small cell lung cancer cells. Biochem Pharmacol 85(3):426–438. doi:10.1016/j.bcp.2012.11.019

Shakarjian MP, Heck DE, Gray JP, Sinko PJ, Gordon MK, Casillas RP, Heindel ND, Gerecke DR, Laskin DL, Laskin JD (2010) Mechanisms mediating the vesicant actions of sulfur mustard after cutaneous exposure. Toxicol Sci 114(1):5–19. doi:10.1093/toxsci/kfp253

Shimomura O, Johnson FH, Morise H (1974) Mechanism of the luminescent intramolecular reaction of aequorin. Biochemistry 13(16):3278–3286. doi:10.1021/bi00713a016

Sies H (1997) Oxidative stress: oxidants and antioxidants. Exp Physiol 82(2):291–295. doi:10.1113/expphysiol.1997.sp004024

Stenger B, Zehfuß F, Mückter H, Schmidt A, Balszuweit F, Schäfer E, Büch T, Gudermann T, Thiermann H, Steinritz D (2014) Activation of the chemosensing transient receptor potential channel A1 (TRPA1) by alkylating agents. Arch Toxicol. doi:10.1007/s00204-014-1414-4

Story GM, Peier AM, Reeve AJ, Eid SR, Mosbacher J, Hricik TR, Earley TJ, Hergarden AC, Andersson DA, Hwang SW, McIntyre P, Jegla T, Bevan S, Patapoutian A (2003) ANKTM1, a TRP-like channel expressed in nociceptive neurons, is activated by cold temperatures. Cell 112(6):819–829. doi:10.1016/S0092-8674(03)00158-2

Sullivan MN, Gonzales AL, Pires PW, Bruhl A, Leo MD, Li W, Oulidi A, Boop FA, Feng Y, Jaggar JH, Welsh DG, Earley S (2015) Localized TRPA1 channel Ca^{2+} signals stimulated by reactive oxygen species promote cerebral artery dilation. Sci Signal 8(358):ra2. doi:10.1126/scisignal.2005659

Thiermann H, Worek F, Kehe K (2013) Limitations and challenges in treatment of acute chemical warfare agent poisoning. Chem Biol Interact 206(3):435–443. doi:10.1016/j.cbi.2013.09.015

Vertuani S, Angusti A, Manfredini S (2004) The antioxidants and pro-antioxidants network: an overview. CPD 10(14):1677–1694. doi:10.2174/1381612043384655

Wang L, Cvetkov TL, Chance MR, Moiseenkova-Bell VY (2012) Identification of in vivo disulfide conformation of TRPA1 ion channel. JBC 287(9):6169–6176. doi:10.1074/jbc.M111.329748

4 Summary and Outlook

Our results demonstrated that TRPA1 channels are activated by the alkylating compounds CEES and SM. Moreover, TRPA1 seems to be substantially linked to the cytotoxicity of these compounds. However, further research on the direct cellular effects of SM-induced and TRPA1-mediated increase of $[Ca^{2+}]_i$ is needed. It is reasonable to assume that Ca^{2+}-dependent signaling pathways are triggered. Previous studies have already connected MAP kinase pathways to TRPA1 activation [68]. CEES exposure has also resulted in a very fast TRPA1-mediated phosphorylation of ERK1/2 that could be prevented by using a specific TRPA1 blocker (Figure 4.1). CEES-induced and presumably TRPA1-mediated cell signaling even results in activation of proteinbiosynthesis as demonstrated by ERK-dependent serum response element (SRE) translocation with subsequent transcription of SRE-regulated genes (Figure 4.1).

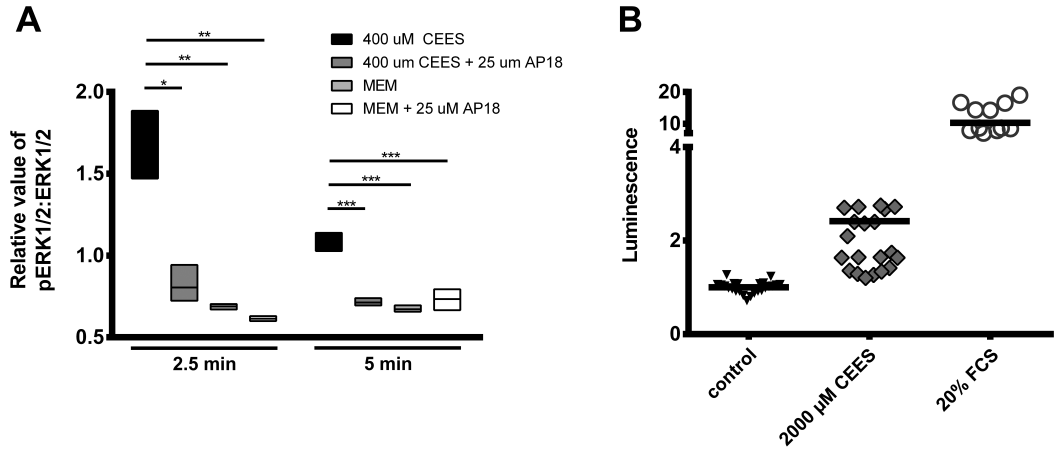

Figure 4.1: Phosphorylation of ERK1/2 and SRE translocation after CEES-exposure. (A) pERK1/2-levels in hTRPA1-overexpressing HEK cells after CEES exposure. A very fast (2.5 min) increase of phosporylated ERK1/2 was detectable. MAPK activation was prevented by inhibiting TRPA1 with the specific blocker AP18. (B) SRE-dependent genes are increased in the same cells 4 h after 2000 μM CEES exposure.

Our findings are supported by other studies that reported MAPK-activation after exposure to alkylating compounds [86, 87, 88]. Ongoing studies using proteomic approaches aim at exploring the cellular sequelae of SM-induced and TRPA1-mediated increase of $[Ca^{2+}]_i$ in more detail.

As stated before, we have proven the capability of alkyating compounds to activate TRPA1 channels. However, the exact mechanism remains unresolved so far. We were able to exclude H^+ and ROS as the major player. TRPA1 can be activated

by covalent modification of intracellular cysteine residues primarily located in the ankyrin repeats. Moreover, channel-modulating properties were described for other cysteine or lysine residues in the TRPA1 protein [59]. Based on our results we assume that extracellular moieties are targeted by SM. This aspect will be investigated in future studies addressing possible covalent modifications of TRPA1 by alkylating compounds. Another study also revealed that not only cysteines within the ankyrin repeat section are important modulators of TRPA1 [89]. TRPA1 mutants, lacking single alkylation sites, are to be established to identify the relevant residues in TRPA1 channels. However, activation of TRPA1 by alkylating compounds may be a combination of different mechanisms, i.e. activation by H^+, ROS, and alkylation of reactive residues (Figure 4.2).

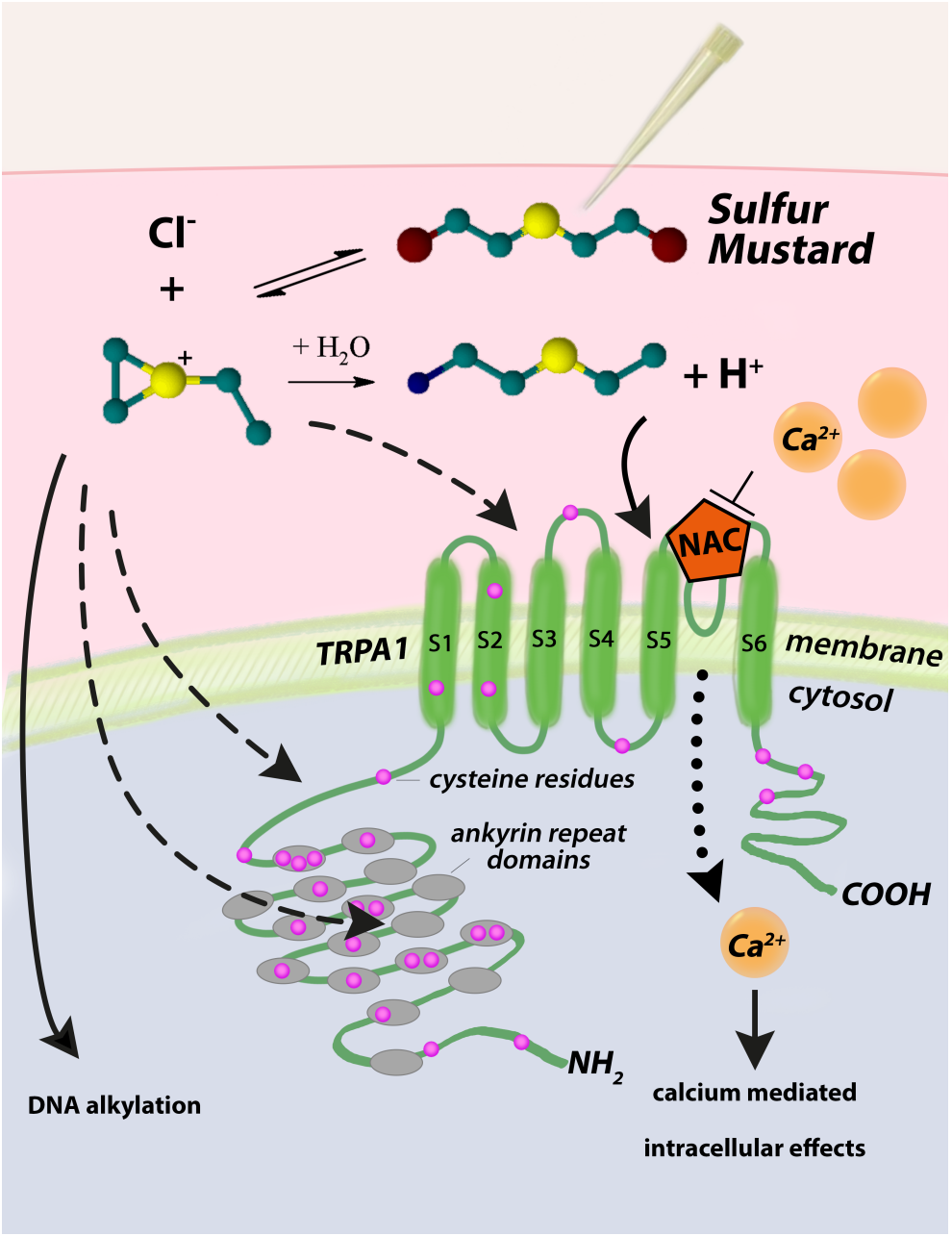

Figure 4.2: Proposed TRPA1 activation by SM.

The role of TRPA1 in SM pathophysiology has to be elucidated. One of the first symptoms patients complain about after SM exposure is tautness in combination with severe itch. Especially, the latter is often resistant to therapy with antihistamines, which are routinely used in histamine-induced pruritus. Histamine-independent itch has also been linked to TRPA1 [90]. Additional symptoms reported after SM exposure include pain, increased inflammation as well as impaired cell proliferation, all of which can be connected to TRPA1-dependent signaling pathways. Thus, TRPA1 blockers – although most likely not a panacea against SM poisoning – may be of benefit to relieve some of the above mentioned symptoms.

5 Bibliography

1. Schnedlitz, M. *Chemische Kampfstoffe: Geschichte, Eigenschaften, Wirkung; Studienarbeit: Zugl.: Wiener Neustadt, FH, Seminararbeit, 2008* 1. Aufl. (GRIN-Verl.Schnedlitz.2008, München, 2008).
2. Freemantle, M. *Gas! Gas! Quick, boys! How chemistry changed the First World War* paperback ed. (History Press, Stroud, 2013).
3. Jankowski, P. *Verdun: The Longest Battle of the Great War* (Oxford University Press USA, Oxford, 2014).
4. Hoenig, S. L. *Handbook of chemical warfare and terrorism* (Greenwood Press, Westport, CT, 2002).
5. Pechura, C. M. & Rall, D. P. *Veterans at Risk: The health effects of mustard gas and Lewisite* (National Academy Press, Washington, D.C, 1993).
6. Fitzgerald, G. J. Chemical warfare and medical response during World War I. *American journal of public health* **98,** 611–625 (2008).
7. *Protocol for the Prohibition of the Use of Asphyxiating, Poisonous or Other Gases, and of Bacteriological Methods of Warfare. Geneva, 17 June 1925*
8. Kaldor, M., Anheier, H. & Glasius, M. *Global civil society 2003* (Oxford University Press, Oxford, 2003).
9. Asserate, A.-W. & Mattioli, A. *Der erste faschistische Vernichtungskrieg: Die italienische Aggression gegen Äthiopien 1935 - 1941 ; [Tagung Der Abessinienkrieg (1935-1941) in Geschichte und Erinnerung, 3. Oktober 2005 an der Universität Luzern]* (SH-Verl., Köln, 2006).
10. Federation of American Scientists. *Uses of CW since the First World War* `https://web.archive.org/web/20100822165939/http://www.fas.org/bwc/papers/review/cwtable.htm`.
11. BBC. *'Chemical Ali' executed in Iraq after Halabja ruling* 25.01.2010. `http://news.bbc.co.uk/2/hi/middle_east/8479115.stm`.
12. Hiltermann, J. R. *A poisonous affair: America, Iraq, and the gassing of Halabja* (Cambridge Univ. Press, Cambridge and New York, NY, 2007).
13. BBC News. *Samples 'confirm IS used mustard agent in Iraq attack'* (ed BBC) 2016. `http://www.bbc.com/news/world-middle-east-35582861`.
14. Grayson, C. A. *From a gassed grandfather to alleged use of chemical weapons by IS... the horrors of mustard gas* 2015. `https://activist1.wordpress.com/2015/09/03/from-a-gassed-grandfather-to-alleged-use-of-chemical-weapons-by-is-the-horrors-of-mustard-gas/`.
15. Balali-Mood, M. & Hefazi, M. The pharmacology, toxicology, and medical treatment of sulphur mustard poisoning. *Fundamental & clinical pharmacology* **19,** 297–315 (2005).
16. Kehe, K. & Szinicz, L. Medical aspects of sulphur mustard poisoning. *Toxicology* **214,** 198–209 (2005).

17. National Institute for Occupational Safety and Health (NIOSH) Education and Information Divisio. *Mustard-Lewisite mixture (HL) : Blister Agent* 20.11.2014. `http://www.cdc.gov/niosh/ershdb/EmergencyResponseCard_29750007.html`.

18. Niemann, A. Ueber die Einwirkung des braunen Chlorschwefels auf Laylgas. *Annalen der Chemie und Pharmazie,* 288–292 (1860).

19. Khateri, S., Ghanei, M., Keshavarz, S., Soroush, M. & Haines, D. Incidence of lung, eye, and skin lesions as late complications in 34,000 Iranians with wartime exposure to mustard agent. *Journal of occupational and environmental medicine* **45,** 1136–1143 (2003).

20. Ghanei, M., Mokhtari, M., Mohammad, M. M. & Aslani, J. Bronchiolitis obliterans following exposure to sulfur mustard: chest high resolution computed tomography. *European journal of radiology* **52,** 164–169 (2004).

21. Ghabili, K., Agutter, P. S., Ghanei, M., Ansarin, K. & Shoja, M. M. Mustard gas toxicity: the acute and chronic pathological effects. *Journal of applied toxicology : JAT* **30,** 627–643 (2010).

22. Taysse, L., Dorandeu, F., Daulon, S., Foquin, A., Perrier, N., Lallement, G. & Breton, P. Cutaneous challenge with chemical warfare agents in the SKH-1 hairless mouse (II): Effects of some currently used skin decontaminants (RSDL and Fuller's earth) against liquid sulphur mustard and VX exposure. *Human & Experimental Toxicology* **30,** 491–498 (June 2011).

23. Shigenobu, T. Occupational cancer of the lungs–cancer of the respiratory tract among workers manufacturing poisonous gases. *Nihon Kyobu Shikkan Gakkai zasshi* **18,** 880–885 (1980).

24. Nishimoto, Y., Yamakido, M., Shigenobu, T., Onari, K. & Yukutake, M. Long-term observation of poison gas workers with special reference to respiratory cancers. *Journal of UOEH* **5 Suppl,** 89–94 (1983).

25. Gilman, A. The initial clinical trial of nitrogen mustard. *American journal of surgery* **105,** 574–578 (1963).

26. Mattes, W. B., Hartley, J. A. & Kohn, K. W. DNA sequence selectivity of guanine-N7 alkylation by nitrogen mustards. *Nucleic acids research* **14,** 2971–2987 (1986).

27. Matijasevic, Z., Precopio, M. L., Snyder, J. E. & Ludlum, D. B. Repair of sulfur mustard-induced DNA damage in mammalian cells measured by a host cell reactivation assay. *Carcinogenesis* **22,** 661–664 (2001).

28. Jowsey, P. A., Williams, F. M. & Blain, P. G. DNA damage responses in cells exposed to sulphur mustard. *Toxicology letters* **209,** 1–10 (2012).

29. Lawley, P. D. & Brookes, P. Interstrand cross-linking of DNA by difunctional alkylating agents. *Journal of Molecular Biology* **25,** 143–160 (1967).

30. Fidder, A., Moes, G. W., Scheffer, A. G., van der Schans, G. P., Baan, R. A., de Jong, L. P. & Benschop, H. P. Synthesis, characterization, and quantitation of the major adducts formed between sulfur mustard and DNA of calf thymus and human blood. *Chemical research in toxicology* **7,** 199–204 (1994).

31. Droge, W. Free radicals in the physiological control of cell function. *Physiological reviews* **82,** 47–95 (2002).

32. Valko, M., Leibfritz, D., Moncol, J., Cronin, M. T. D., Mazur, M. & Telser, J. Free radicals and antioxidants in normal physiological functions and human disease. *The international journal of biochemistry & cell biology* **39,** 44–84 (2007).

33. Paromov, V., Suntres, Z., Smith, M. & Stone, W. L. Sulfur mustard toxicity following dermal exposure: role of oxidative stress, and antioxidant therapy. *Journal of burns and wounds* **7,** e7 (2007).

34. Husain, K., Dube, S. N., Sugendran, K., Singh, R., Das Gupta, S. & Somani, S. M. Effect of topically applied sulphur mustard on antioxidant enzymes in blood cells and body tissues of rats. *Journal of applied toxicology : JAT* **16,** 245–248 (1996).

35. Pacher, P., Beckman, J. S. & Liaudet, L. Nitric oxide and peroxynitrite in health and disease. *Physiological reviews* **87,** 315–424 (2007).

36. Vanden Berghe, T., Linkermann, A., Jouan-Lanhouet, S., Walczak, H. & Vandenabeele, P. Regulated necrosis: the expanding network of non-apoptotic cell death pathways. *Nature reviews. Molecular cell biology* **15,** 135–147 (2014).

37. Reggiori, F. & Klionsky, D. J. Autophagy in the eukaryotic cell. *Eukaryotic cell* **1,** 11–21 (2002).

38. Green, D. R. *Means to an end: Apoptosis and other cell death mechanisms* (Cold Spring Harbor Laboratory Pr, Cold Spring Harbor, NY, 2011).

39. Green, D. R. & Llambi, F. Cell Death Signaling. *Cold Spring Harbor perspectives in biology* **7** (2015).

40. deCathelineau, A. M. & Henson, P. M. The final step in programmed cell death: phagocytes carry apoptotic cells to the grave. *Essays in biochemistry* **39,** 105–117 (2003).

41. Vandivier, R. W., Henson, P. M. & Douglas, I. S. Burying the dead: the impact of failed apoptotic cell removal (efferocytosis) on chronic inflammatory lung disease. *Chest* **129,** 1673–1682 (2006).

42. Rosenthal, D. S., Simbulan-Rosenthal, C. M., Iyer, S., Spoonde, A., Smith, W., Ray, R. & Smulson, M. E. Sulfur mustard induces markers of terminal differentiation and apoptosis in keratinocytes via a Ca2+-calmodulin and caspase-dependent pathway. *The Journal of investigative dermatology* **111,** 64–71 (1998).

43. Steinritz, D., Emmler, J., Hintz, M., Worek, F., Kreppel, H., Szinicz, L. & Kehe, K. Apoptosis in sulfur mustard treated A549 cell cultures. *Life sciences* **80,** 2199–2201 (2007).

44. Kehe, K., Balszuweit, F., Steinritz, D. & Thiermann, H. Molecular toxicology of sulfur mustard-induced cutaneous inflammation and blistering. *Toxicology* **263,** 12–19 (2009).

45. Ray, R., Simbulan-Rosenthal, C. M., Keyser, B. M., Benton, B., Anderson, D., Holmes, W., Trabosh, V. A., Daher, A. & Rosenthal, D. S. Sulfur mustard induces apoptosis in lung epithelial cells via a caspase amplification loop. *Toxicology* **271,** 94–99 (2010).

46. Arroyo, C. M., Schafer, R. J., Kurt, E. M., Broomfield, C. A. & Carmichael, A. J. Response of normal human keratinocytes to sulfur mustard (HD): cytokine release using a non-enzymatic detachment procedure. *Human & experimental toxicology* **18,** 1–11 (1999).

47. Tewari-Singh, N., Jain, A. K., Inturi, S., Agarwal, C., White, C. W. & Agarwal, R. Silibinin attenuates sulfur mustard analog-induced skin injury by targeting multiple pathways connecting oxidative stress and inflammation. *PloS one* **7,** e46149 (2012).

48. United States Army Chemical Corps Museum Shop. *Air Poster Series: Training AIDS Division*

49. US Army. *World War II Gas Identification Posters, ca. 1941-1945* 21.12.2011. `http://nmhm.washingtondc.museum/collections/archives/agalleries/ww2/mustard_gas.jpg`.

50. Bessac, B. F. & Jordt, S.-E. Sensory detection and responses to toxic gases: mechanisms, health effects, and countermeasures. *Proceedings of the American Thoracic Society* **7,** 269–277 (2010).

51. Gonzalez, C., Almaraz, L., Obeso, A. & Rigual, R. Carotid body chemoreceptors: from natural stimuli to sensory discharges. *Physiological reviews* **74,** 829–898 (1994).

52. Bessac, B. F., Sivula, M., von Hehn, C. A., Escalera, J., Cohn, L. & Jordt, S.-E. TRPA1 is a major oxidant sensor in murine airway sensory neurons. *The Journal of clinical investigation* **118,** 1899–1910 (2008).

53. Clapham, D. E. TRP channels as cellular sensors. *Nature* **426,** 517–524 (2003).

54. *Transient receptor potential (TRP) channels* (ed Flockerzi, V. M.) (Springer, Berlin, 2007).

55. Kalia, J. & Swartz, K. J. Exploring structure-function relationships between TRP and Kv channels. *Scientific reports* **3,** 1523 (2013).

56. Paulsen, C. E., Armache, J.-P., Gao, Y., Cheng, Y. & Julius, D. Structure of the TRPA1 ion channel suggests regulatory mechanisms. *Nature* **520,** 511–517 (2015).

57. Hardie, R. C. & Minke, B. The trp gene is essential for a light-activated Ca2+ channel in Drosophila photoreceptors. *Neuron* **8,** 643–651 (1992).

58. Bautista, D. M., Siemens, J., Glazer, J. M., Tsuruda, P. R., Basbaum, A. I., Stucky, C. L., Jordt, S.-E. & Julius, D. The menthol receptor TRPM8 is the principal detector of environmental cold. *Nature* **448,** 204–208 (2007).

59. Bessac, B. F. & Jordt, S.-E. Breathtaking TRP channels: TRPA1 and TRPV1 in airway chemosensation and reflex control. *Physiology* **23,** 360–370 (2008).

60. Ishimaru, Y. & Matsunami, H. Transient receptor potential (TRP) channels and taste sensation. *Journal of dental research* **88,** 212–218 (2009).

61. Hill-Eubanks, D. C., Gonzales, A. L., Sonkusare, S. K. & Nelson, M. T. Vascular TRP channels: performing under pressure and going with the flow. *Physiology* **29,** 343–360 (2014).

62. Nilius, B., Appendino, G. & Owsianik, G. The transient receptor potential channel TRPA1: from gene to pathophysiology. *Pflugers Archiv : European journal of physiology* **464,** 425–458 (2012).

63. Shigetomi, E., Jackson-Weaver, O., Huckstepp, R. T., O'Dell, T. J. & Khakh, B. S. TRPA1 channels are regulators of astrocyte basal calcium levels and long-term potentiation via constitutive D-serine release. *The Journal of neuroscience* **33,** 10143–10153 (2013).

64. Fernandes, E. S., Fernandes, M. A. & Keeble, J. E. The functions of TRPA1 and TRPV1: moving away from sensory nerves. *British journal of pharmacology* **166,** 510–521 (2012).

65. Laursen, W. J., Bagriantsev, S. N. & Gracheva, E. O. TRPA1 channels: chemical and temperature sensitivity. *Current topics in membranes* **74,** 89–112 (2014).

66. Macpherson, L. J., Dubin, A. E., Evans, M. J., Marr, F., Schultz, P. G., Cravatt, B. F. & Patapoutian, A. Noxious compounds activate TRPA1 ion channels through covalent modification of cysteines. *Nature* **445,** 541–545 (2007).

67. Bessac, B. F., Sivula, M., von Hehn, C. A., Caceres, A. I., Escalera, J. & Jordt, S.-E. Transient receptor potential ankyrin 1 antagonists block the noxious effects of toxic industrial isocyanates and tear gases. *FASEB journal* **23,** 1102–1114 (2009).

68. Buech, T. R. H., Schafer, E. A. M., Demmel, M.-T., Boekhoff, I., Thiermann, H., Gudermann, T., Steinritz, D. & Schmidt, A. Functional expression of the transient receptor potential channel TRPA1, a sensor for toxic lung inhalants, in pulmonary epithelial cells. *Chemico-biological interactions* **206,** 462–471 (2013).

69. John, H., Siegert, M., Gandor, F., Gawlik, M., Kranawetvogl, A., Karaghiosoff, K. & Thiermann, H. Optimized verification method for detection of an albumin-sulfur mustard adduct at Cys(34) using a hybrid quadrupole time-of-flight tandem mass spectrometer after direct plasma proteolysis. *Toxicology letters* **244,** 103–111 (2016).

70. Steinritz, D., Striepling, E., Rudolf, K.-D., Schroder-Kraft, C., Puschel, K., Hullard-Pulstinger, A., Koller, M., Thiermann, H., Gandor, F., Gawlik, M. & John, H. Medical documentation, bioanalytical evidence of an accidental human exposure to sulfur mustard and general therapy recommendations. *Toxicology letters* **244,** 112–120 (2016).

71. Gandor, F., Gawlik, M., Thiermann, H. & John, H. Evidence of Sulfur Mustard Exposure in Human Plasma by LC-ESI-MS-MS Detection of the Albumin-Derived Alkylated HETE-CP Dipeptide and Chromatographic Investigation of Its Cis/Trans Isomerism. *Journal of analytical toxicology* **39,** 270–279 (2015).

72. Kendall, J. M. & Badminton, M. N. Aequorea victoria bioluminescence moves into an exciting new era. *Trends in biotechnology* **16,** 216–224 (1998).

73. Shimomura, O., Johnson, F. H. & Saiga, Y. Extraction, purification and properties of aequorin, a bioluminescent protein from the luminous hydromedusan, Aequorea. *Journal of cellular and comparative physiology* **59,** 223–239 (1962).

74. De La Roche, J., Eberhardt, M. J., Klinger, A. B., Stanslowsky, N., Wegner, F., Koppert, W., Reeh, P. W., Lampert, A., Fischer, M. J. M. & Leffler, A. The molecular basis for species-specific activation of human TRPA1 protein by protons involves poorly conserved residues within transmembrane domains 5 and 6. *The Journal of biological chemistry* **288,** 20280–20292 (2013).

75. Wang, Y. Y., Chang, R. B., Allgood, S. D., Silver, W. L. & Liman, E. R. A TRPA1-dependent mechanism for the pungent sensation of weak acids. *The Journal of general physiology* **137,** 493–505 (2011).

76. Naghii, M. R. Sulfur mustard intoxication, oxidative stress, and antioxidants. *Military medicine* **167,** 573–575 (2002).

77. Korkmaz, A., Yaren, H., Topal, T. & Oter, S. Molecular targets against mustard toxicity: implication of cell surface receptors, peroxynitrite production, and PARP activation. *Archives of toxicology* **80,** 662–670 (2006).

78. Steinritz, D., Elischer, A., Balszuweit, F., Gonder, S., Heinrich, A., Bloch, W., Thiermann, H. & Kehe, K. Sulphur mustard induces time- and concentration-dependent regulation of NO-synthesizing enzymes. *Toxicology letters* **188,** 263–269 (2009).

79. Steinritz, D., Schmidt, A., Simons, T., Ibrahim, M., Morguet, C., Balszuweit, F., Thiermann, H., Kehe, K., Bloch, W. & Bolck, B. Chlorambucil (nitrogen mustard) induced impairment of early vascular endothelial cell migration - effects of alpha-linolenic acid and N-acetylcysteine. *Chemico-biological interactions* **219,** 143–150 (2014).

80. Lin, A.-H., Liu, M.-H., Ko, H.-K., Perng, D.-W., Lee, T.-S. & Kou, Y. R. Lung Epithelial TRPA1 Transduces the Extracellular ROS into Transcriptional Regulation of Lung Inflammation Induced by Cigarette Smoke: The Role of Influxed Ca(2+). *Mediators of inflammation* **2015,** 148367 (2015).

81. Lin, Y. S., Hsu, C.-C., Bien, M.-Y., Hsu, H.-C., Weng, H.-T. & Kou, Y. R. Activations of TRPA1 and P2X receptors are important in ROS-mediated stimulation of capsaicin-sensitive lung vagal afferents by cigarette smoke in rats. *Journal of applied physiology* **108,** 1293–1303 (2010).

82. Taylor-Clark, T. E. & Undem, B. J. Sensing pulmonary oxidative stress by lung vagal afferents. *Respiratory physiology & neurobiology* **178,** 406–413 (2011).

83. Rushworth, G. F. & Megson, I. L. Existing and potential therapeutic uses for N-acetylcysteine: the need for conversion to intracellular glutathione for antioxidant benefits. *Pharmacology & therapeutics* **141,** 150–159 (2014).

84. Santangelo, F. Intracellular thiol concentration modulating inflammatory response: influence on the regulation of cell functions through cysteine prodrug approach. *Current medicinal chemistry* **10,** 2599–2610 (2003).

85. Mangerich, A., Debiak, M., Birtel, M., Ponath, V., Balszuweit, F., Lex, K., Martello, R., Burckhardt-Boer, W., Strobelt, R., Siegert, M., Thiermann, H., Steinritz, D., Schmidt, A. & Burkle, A. Sulfur and nitrogen mustards induce characteristic poly(ADP-ribosyl)ation responses in HaCaT keratinocytes with distinctive cellular consequences. *Toxicology letters* **244,** 56–71 (2016).

86. Kumar, D., Tewari-Singh, N., Agarwal, C., Jain, A. K., Inturi, S., Kant, R., White, C. W. & Agarwal, R. Nitrogen mustard exposure of murine skin induces DNA damage, oxidative stress and activation of MAPK/Akt-AP1 pathway leading to induction of inflammatory and proteolytic mediators. *Toxicology letters* **235,** 161–171 (2015).

87. Yego, E. C. K. & Dillman, J. F. 3. Cytokine regulation by MAPK activated kinase 2 in keratinocytes exposed to sulfur mustard. *Toxicology in vitro* **27,** 2067–2075 (2013).

88. Popp, T., Egea, V., Kehe, K., Steinritz, D., Schmidt, A., Jochum, M. & Ries, C. Sulfur mustard induces differentiation in human primary keratinocytes: opposite roles of p38 and ERK1/2 MAPK. *Toxicology letters* **204,** 43–51 (2011).

89. Survery, S., Moparthi, L., Kjellbom, P., Hogestatt, E. D., Zygmunt, P. M. & Johanson, U. The N-terminal Ankyrin Repeat Domain Is Not Required for Electrophile and Heat Activation of the Purified Mosquito TRPA1 Receptor. *The Journal of biological chemistry* (2016).

90. Wilson, S. R., Gerhold, K. A., Bifolck-Fisher, A., Liu, Q., Patel, K. N., Dong, X. & Bautista, D. M. TRPA1 is required for histamine-independent, Mas-related G protein-coupled receptor-mediated itch. *Nature neuroscience* **14,** 595–602 (2011).